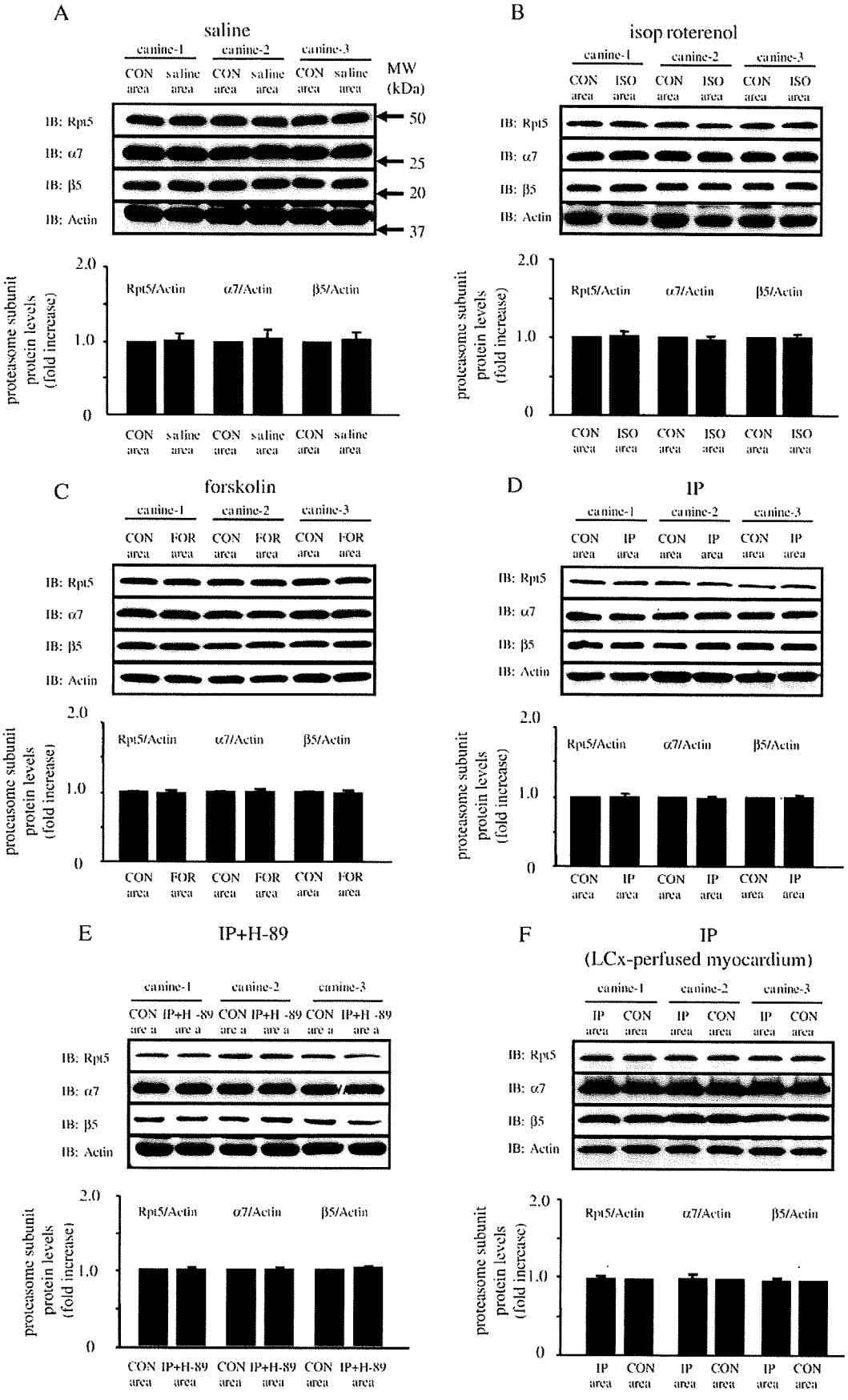
A
saline
canine-1
canine-2
canine-3
CON area
saline area
MW (kDa)
IB: Rpt5
IB: α7
IB: β5
IB: Actin
50
25
20
37
proteasome subunit protein levels (fold increase)
Rpt5/Actin
α7/Actin
β5/Actin
B
isop roterenol
ISO area
C
forskolin
FOR area
D
IP
IP area
E
IP+H-89
IP+H -89 are a
F
IP
(LCx-perfused myocardium)

2.5.4. Protocol IV: Effects of proteasome activation by IP on the accumulation of ubiquitinated proteins and infarct size in canine hearts

To assess pathophysiological roles of the proteasome in the ischemia/reperfusion myocardium, we intracoronarilly administered saline (n=9) or a proteasome inhibitor (epoxomicin at 2.5 μg/kg) (n=7) for 50 min and then we performed 90 min of ischemia followed by 6 h of reperfusion in dogs. To assess pathophysiological roles of the proteasome activation by IP in the ischemic/reperfused myocardium, we intracoronarilly administered a proteasome inhibitor (epoxomicin at 2.5 μg/kg) for 50 min with (n=7) and without IP (n=9) and then we performed 90 min of ischemia followed by 6 h of reperfusion in dogs. We preliminarily confirmed that this dose of epoxomicin reduced 26S proteasome activity by 43.0±6.2% (n=3) in the LAD-perfused myocardium compared with that in the LCx-perfused one. After 6 h of reperfusion, we rapidly sampled LAD-perfused myocardium, stored the samples at −80 °C, and investigated the level of the ubiquitinated proteins. We also evaluated the area at risk and the necrotic area after 6 h of reperfusion by Evans blue/TTC staining as described previously [19]. Myocardial infarct size was expressed as the necrotic area/area at risk (Fig. 1).

2.6. Purification of cardiac proteasome

Proteasome was purified from canine hearts according the method reported previously [20]. The peptidase assay was performed using the cytosolic fraction from the LAD- and LCx-perfused myocardium of canine hearts or the fractions containing 26S proteasomes separated on a 10–40% glycerol gradient centrifugation according to the method described above.

2.7. Western blotting analysis

Western blotting analysis was performed as described previously [21]. Immunoreactive bands were quantified by densitometry (Molecular Dynamics).

2.8. Statistical analysis

Data are expressed as the mean±SEM. Proteasome activities in LAD- and LCx-perfused myocardium were compared by the paired t-test. The time-course changes in proteasome activity during ischemia/reperfusion myocardium were analyzed by the two-way repeated analysis of variance (ANOVA) followed by Fisher's test. Other results were compared by the one-factor ANOVA followed by Fisher's test. In all analyses, $p<0.05$ was accepted as statistically significant.

3. Results

3.1. PKA enhanced the activity of purified 26S proteasome

The in vitro peptidase assay (Fig. 2A) and the in-gel peptidase assays (Figs. 2B, C) showed that the treatment of purified 26S proteasome with PKA enhanced 26S proteasome activity in a dose-dependent manner, while this effect was blocked by the pretreatment with H-89.

3.2. PKA enhanced the phosphorylation and assembly of purified 26S proteasome

Western blotting analysis of non-reducing gels probed with the antibody against serine/threonine phosphorylated proteins showed that PKA dose-dependently enhanced the phosphorylation of purified 26S proteasome (Figs. 3A, B). The phosphorylation of 26S proteasome was blocked by the pretreatment with H-89 (Figs. 3A, B). Interestingly, Western blotting analysis of non-reducing gels probed with the antibody against Rpt5 or α7 revealed that PKA dose-dependently increased either protein level that corresponded to 26S proteasome, which was blunted by H-89 (Figs. 3C, D upper panel). Western blotting analysis of reducing gels showed that the purified 26S proteasome were equally loaded to each lane (Figs. 3C, D lower panel). These results suggest that PKA enhanced the phosphorylation and assembly of proteasome, which may lead to the increase in proteasome activity.

3.3. PKA stimulation increased 26S proteasome activity in canine hearts

We found no differences in the proteasome activity in the saline-treated (LAD-perfused) and the control (LCx-perfused) myocardium (Fig. 4A). In contrast, exogenous and endogenous PKA stimulation by the selective intracoronary administration of isoproterenol or forskolin and IP, respectively, significantly increased 26S proteasome activity in LAD-perfused myocardium compared with that in LCx-perfused one (Figs. 4B, C, D). The selective intracoronary administration of a PKA inhibitor, H-89, blocked proteasome activation by IP (Fig. 4E). We confirmed that proteasome activation by IP in LCx-perfused myocardium was the same as that in LAD-perfused one (Fig. 4F). These results suggest that exogenous and endogenous PKA stimulation increased 26S proteasome activity in canine hearts.

3.4. PKA stimulation did not alter total protein levels of proteasome subunits in canine hearts

We found no differences in the total protein levels of proteasome subunits in the saline-treated (LAD-perfused) and the control (LCx-perfused) myocardium (Fig. 5A). Then, we examined the changes in protein levels of the proteasome subunits such as Rpt5, α7 and β5 in LAD- and LCx-perfused myocardium when proteasome was activated by exogenous and endogenous PKA stimulation in canine hearts. Importantly, there were no differences in the total protein levels of 3 proteasome subunits (Rpt5, α7, β5) in groups tested (Figs. 5B–F). These results suggest that exogenous and endogenous PKA stimulation did not alter total protein levels of proteasome subunits in the in vivo canine hearts.

3.5. PKA stimulation enhanced 26S proteasome activity and assembly in canine hearts

Since we found 26S proteasome activity of canine hearts mainly in the fractions 17–19 after glycerol gradient centrifugation (Figs. 6A–F, upper panels), samples from fractions 15–21 in the LCx- and LAD-perfused myocardium were immunoblotted with antibodies against Rpt5, α7 or β5 (Figs. 6A–F, lower panels). Consistently, Western blotting analysis with SDS-PAGE gel showed that proteasome subunit Rpt5, α7 or β5 was found mainly in fractions 17–19 (Figs. 6A–F, lower panels).

Fig. 6. Exogenous and endogenous PKA stimulation enhanced 26S proteasome assembly in canine hearts. Representative analysis of 26S proteasome activity (upper panel) and Western blotting analysis of proteasome subunits (lower panel) in the control and treated myocardium. The number indicated fractions separated on a 10–40% glycerol gradient centrifugation. (A) saline, (B) isoproterenol (ISO), (C) forskolin (FOR), (D) ischemic preconditioning (IP), (E) IP with H-89 (IP+H-89), (F) IP in LCx-perfused myocardium. (G) Quantitative analysis of 26S proteasome activity in canine hearts. Proteasome activity was expressed as the summation of proteasome activity in fractions 17–19 in the treatment myocardium which were divided by that in the same fractions in the control one (n=4 to 8 each). (H) Quantitative analysis of proteasome assembly in canine hearts. Proteasome assembly was expressed as the summation of Rpt5 protein levels in fractions 17–19 in the treatment myocardium which were divided by that in the same fractions in the control ones (n=4 to 8 each). *$p<0.05$ vs sham. #$p<0.05$ vs IP+H-89.

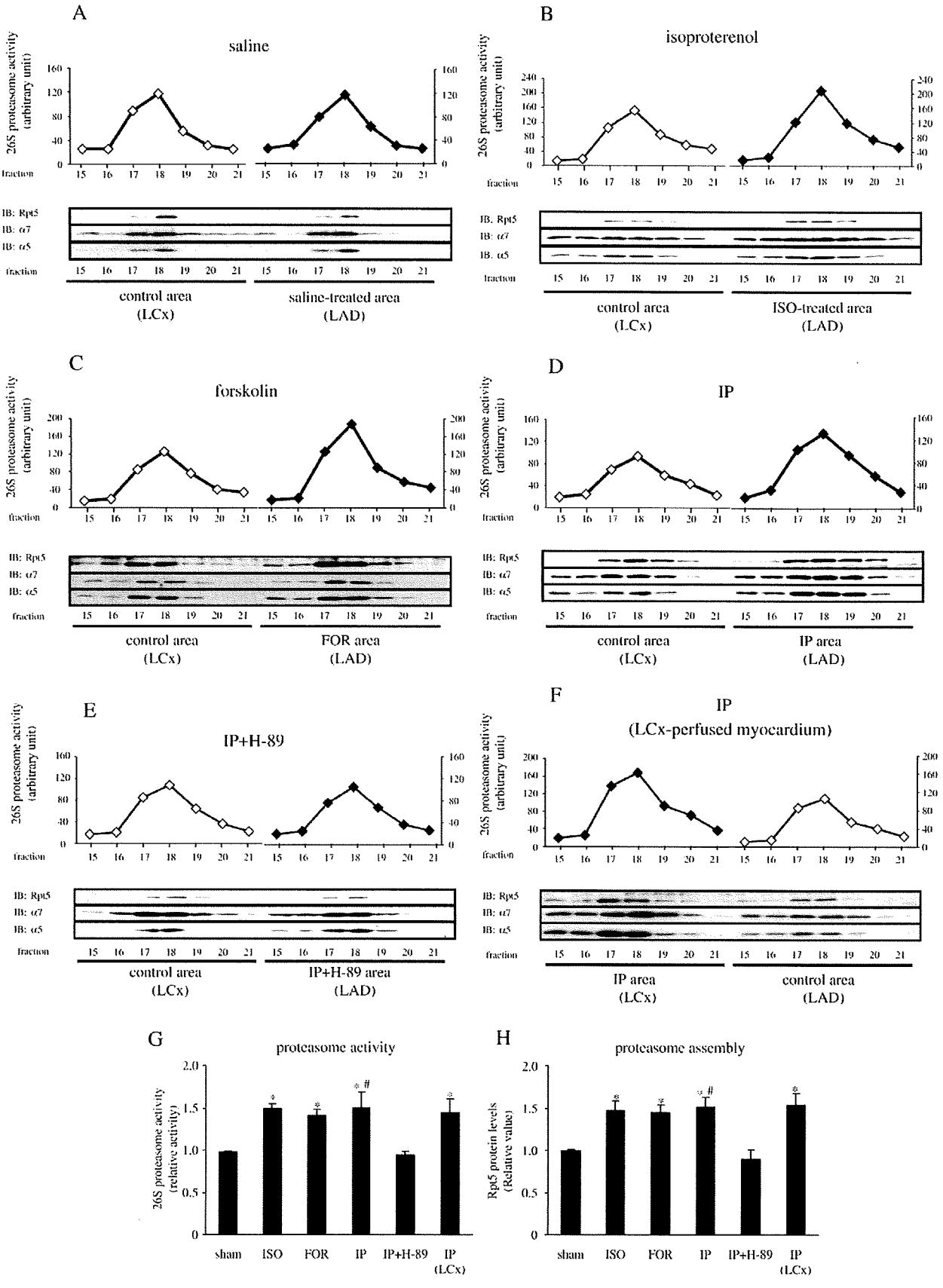
A
saline
26S proteasome activity (arbitrary unit)
fraction
IB: Rpt5
IB: α7
IB: α5
control area (LCx)
saline-treated area (LAD)
B
isoproterenol
control area (LCx)
ISO-treated area (LAD)
C
forskolin
control area (LCx)
FOR area (LAD)
D
IP
control area (LCx)
IP area (LAD)
E
IP+H-89
control area (LCx)
IP+H-89 area (LAD)
F
IP
(LCx-perfused myocardium)
IP area (LCx)
control area (LAD)
G
proteasome activity
26S proteasome activity (relative activity)
sham
ISO
FOR
IP
IP+H-89
IP (LCx)
H
proteasome assembly
Rpt5 protein levels (Relative value)

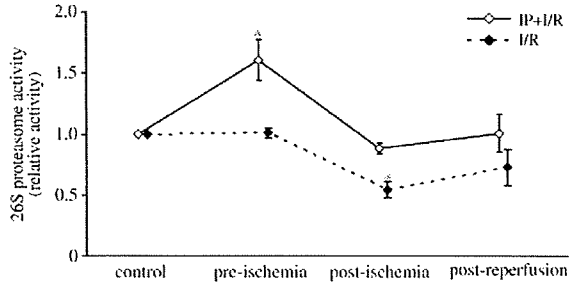

Fig. 7. Time-course changes in proteasome activity during ischemia/reperfusion period. Proteasome activity during ischemia/reperfusion period with and without IP. Myocardial biopsy specimens were taken at the control, just before ischemia (pre-ischemia), at the end of 90 min of ischemia (post-ischemia) and 6 h of reperfusion (post-reperfusion). Proteasome activity in IP+I/R and I/R groups was normalized to the corresponding control ones. IP+I/R and I/R indicate ischemia/reperfusion with and without IP, respectively. *$p<0.05$ vs control at the corresponding group.

Fig. 6 showed the representative proteasome activity and assembly using the myocardial sample of canine-1 in each groups in Fig. 5. Since we confirmed that the total amount of proteasome subunits were same in the control and treated myocardium, the alteration in protein levels of proteasome subunits in proteasome enriched fractions 17–19 indicate the alternation in the status of proteasome assembly. No differences were found in protein levels of proteasome subunits in the saline-treated (LAD-perfused) and the control (LCx-perfused) myocardium (Fig. 6A). Importantly, along with the increase in proteasome activity, the exogenous and endogenous PKA stimulation by isoproterenol, forskolin and IP significantly increased the protein levels of 3 different proteasome subunits in fractions 17–19 in the LAD-perfused myocardium compared with those in LCx-perfused one (Figs. 6B–D). Moreover, the selective administration of H-89 blunted the increases in protein levels of 3 different proteasome subunits and proteasome activation by IP in fractions 17–19 in the LAD-perfused myocardium (Fig. 6E). We also confirmed that the same findings were induced by IP in LCx-perfused myocardium (Fig. 6F). Quantitative analysis also showed that PKA enhanced proteasome activity and assembly, both of which were expressed as the summation of proteasome activity and Rpt5 protein levels in fractions 17–19 in the treatment myocardium which were divided by that in the same fractions in the control one, respectively (Figs. 6G, H). These results suggest that PKA stimulation enhanced 26S proteasome assembly and activity in canine hearts without alteration of total protein levels of proteasome subunits.

3.6. Time-course changes in proteasome activity during ischemia/reperfusion period with and without IP

The analysis of consecutive myocardial biopsy samples also revealed that IP increased the proteasome activity in the LAD-perfused myocardium in the same dog (Fig. 7). In canine hearts with IP, the proteasome activities at the post-ischemia and post-reperfusion were significantly lower than that at the pre-ischemia (=just after IP), but they did not differ from the control. In canine hearts without IP, the proteasome activity at the post-ischemia was significantly decreased compared with that at the control or pre-ischemia (Fig. 7). Myocardial proteasome activity at the post-reperfusion did not differ from that at the post-ischemia in groups with and without IP (Fig. 7).

3.7. IP blunted the accumulation of ubiquitinated proteins in ischemia/reperfusion myocardium

To examine the pathophysiological role of proteasome activation by IP, we investigated effects of IP on the accumulation of ubiquitinated proteins, which may predict recovery of postischemic cardiac function [22], in the ischemia/reperfusion myocardium in canine model. Western blotting analysis revealed that ubiquitinated proteins were increased in ischemia/reperfusion myocardium, while their accumulation was attenuated by IP (Figs. 8A, B). The reduction in

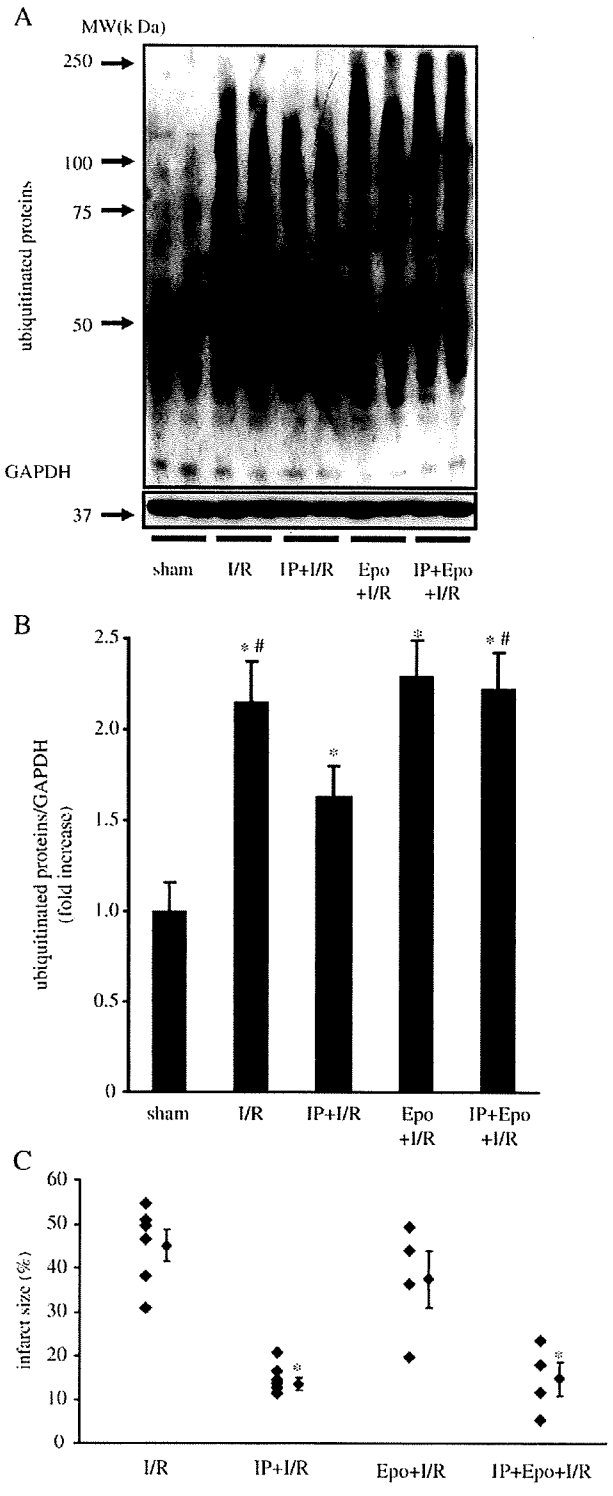

Fig. 8. Pathophysiological role of the enhancement of proteasome activity by IP. Representative example (A) and quantitative analysis (B) of Western blotting analysis of ubiquitinated proteins in canine ischemia/reperfusion (I/R) myocardium. *$p<0.05$ vs. sham, #$p<0.05$ vs. IP+I/R. $n=3$ per group. Values were normalized to sham. (C) Myocardial infarct size. *$p<0.05$ vs. I/R. MW, IP and Epo indicate molecular weight, ischemic preconditioning and epoxomicin (a proteasome inhibitor), respectively.

accumulated ubiquitinated proteins by IP was blunted by a proteasome inhibitor, epoxomicin. These results indicate that proteasome activation by IP alleviated the accumulation of ubiquitinated proteins in canine ischemia/reperfusion hearts.

3.8. Proteasome inhibition did not alter infarct size in canine hearts with and without IP

Fig. 8C showed the infarct size for each group in protocol IV. The intracoronary administration of epoxomicin before ischemia did not alter infarct size in this canine model. Consistent with the previous reports [15], we found that IP reduced myocardial infarct size. The infarct size-limiting effects of IP were not affected by the intracoronary administration of epoxomicin during IP procedure.

4. Discussion

4.1. PKA rapidly enhances phosphorylation, assembly and activity of 26S purified proteasome

Proteasome regulates cellular functions by eliminating ubiquitinated proteins [1–4]. Proteasome activity is enhanced by an increase in the levels of proteasome subunit proteins and their assembly, as well as by the post-translational modification of proteasome subunit through processes such as phosphorylation/dephosphorylation [9,10]. Recent studies have shown that PKA can phosphorylate several sites and increase proteasome activity in vitro [11,12]. Furthermore, although the involvement of PKA is not shown, the phosphorylation of proteasome subunits alters the status of proteasome assembly [23,24]. In the present study, we firstly showed that PKA activation enhanced the proteasome assembly, which contributed to the increase in proteasome activity. These findings suggest that altering proteasome subunit configuration through directed assembly by PKA may lead to the increase in proteasome activity, although we cannot exclude the possibility that PKA-mediated phosphorylation of proteasome subunits directly activates proteasome. Further investigation will be needed to clarify what subunit of proteasome is phosphorylated by PKA and the direct association between phosphorylation and assembly.

4.2. PKA stimulation enhances assembly and activity in in vivo canine hearts without affecting the total protein levels of proteasome subunits

Since proteasome activity is regulated by the multiple factors such as intracellular ATP levels and post-translational modification of proteasome [9,10], the in vitro findings of proteasome regulation are not always applied in the vivo model. Thus, to clarify whether the in vitro findings were also valid in vivo, we examined whether PKA stimulation could modulate proteasome assembly and activity in canine hearts. We employed two maneuvers to activate PKA in vivo, which were isoproterenol and forskolin as an exogenous stimulant of PKA [18,25] and IP as an endogenous stimulant [15]. We confirmed that both exogenous and endogenous stimulation of PKA enhanced 26S proteasome activity at 30 min after administration without changing the total protein levels of proteasome subunits in in vivo canine hearts. To our knowledge, the present study is the first to show the intervention to increase proteasome activity in vivo, suggesting that the pathophysiological conditions due to proteasome dysfunction in hearts could be treated.

We have found both 20S (α7 and β5) and 19S (Rpt5) subunit proteins in fractions where proteasome activity was detected, indicating that 26S proteasome was indeed eluted in these fractions. We confirmed that exogenous and endogenous PKA stimulation increased the protein levels of proteasome subunits in these fractions without changing total amount of proteasome subunits. These findings suggest that PKA stimulation enhanced 26S proteasome assembly as well as activity in in vivo canine hearts.

4.3. Time-course changes in proteasome activity during ischemia/reperfusion period with and without IP

To examine the time-course changes in proteasome activity during ischemia/reperfusion period, we performed myocardial biopsy at 4 time-points during ischemia/reperfusion period: at the control, just before ischemia (pre-ischemia), at the end of 90 min ischemia (post-ischemia) and 6 h of reperfusion (post-reperfusion). Previous study indicated that proteasome activity was decreased after ischemia/reperfusion [8]. Consistent with the previous report, the proteasome activity at the post-ischemia was significantly decreased compared with that at the control or pre-ischemia in groups without IP. Meanwhile, the proteasome activity at the post-ischemia was significantly lower than that at the pre-ischemia (=just after IP), however, it did not differ from the control in groups with IP (Fig. 7). These findings suggest that stimuli during ischemic period decreased myocardial proteasome activity and that proteasome activation by IP during ischemic period may play an important role in the protein turnover and cellular functions in ischemia/reperfusion hearts. Myocardial proteasome activity at the end of reperfusion did not differ from that at the end of ischemia in groups with and without IP, suggesting that stimuli during reperfusion did not significantly affect proteasome activity. Unfortunately, due to the small volume of biopsy samples, we could not check the time-course changes in the status of proteasome assembly.

4.4. IP blunts the accumulation of ubiquitinated proteins in ischemia/reperfusion myocardium

Recently, the ubiquitination of proteins is important post-translational processes that modify the functions of many proteins. We and others have reported that the accumulation of ubiquitinated protein in hearts was associated with the progression of cardiac dysfunction due to apoptosis [7,26]. In addition, the injured myocardium by ischemia/reperfusion is concomitant with a reduced proteasome activity [8]. Consistent with these previous reports, we found the decreased proteasome activity and the accumulation of ubiquitinated proteins in the ischemia/reperfusion myocardium. Interestingly, we found the less accumulation of ubiquitinated proteins in ischemia/reperfusion myocardium, which may be attributable to the 40% increase in proteasome activity by endogenous PKA stimulation. Since the accumulation of ubiquitinated proteins may predict recovery of postischemic cardiac function [21], the removal of damaged proteins due to proteasome activation by IP may contribute to improve postischemic cardiac function.

4.5. Proteasome inhibition did not alter infarct size in canine hearts with and without IP

Finally, we examined whether proteasome activation by IP contributed to its infarct-size limiting effects in the canine model. The infarct-size limiting effects of IP were not prevented by the intracoronary administration of epoxomicin, a proteasome inhibitor, at the dose that reduces proteasome activity by 43%. These findings suggest that proteasome activation by IP was not involved in the infarct-size limiting effects of IP in the acute phase. Future studies will be required about the pathophysiological role of proteasome activation in the chronic phase after myocardial infarction. Moreover, the intracoronary administration of epoxomicin itself could not reduce the infarct size in this model. This data was inconsistent with the previous ones that the inhibition of proteasome could reduce myocardial infarct size in rats and pigs [27,28]. The discrepancy between the previous and our studies might be due to the differences in animals used, experimental protocols and the drugs used. Further investigation will be needed to clarify whether reduced proteasome activity is beneficial or detrimental in the ischemia/reperfusion injury in the acute phase.

In conclusion, the present study demonstrated that PKA rapidly enhances proteasome activity and assembly in the in vivo heart. Modulation of proteasome activity and assembly might be a promising new therapeutic approach for cardiovascular diseases.

Acknowledgments

We thank Saori Ikezawa and Yoko Hamada for their technical assistance, and Kieko Segawa for the secretarial work. This work is supported by Grants-in-aid from the Ministry of Health, Labor, and Welfare-Japan and Grants-in-aid from the Ministry of Education, Culture, Sports, Science and Technology-Japan and Grants from the Japan Heart Foundation and Grants from the Japan Cardiovascular Research Foundation.

References

[1] Hershko A, Ciechanover A. The ubiquitin system. Annu Rev Biochem 1998;67:425–79.
[2] Hochstrasser M. Ubiquitin, proteasomes, and the regulation of intracellular protein degradation. Curr Opin Cell Biol 1995;7:215–23.
[3] Glickman MH, Ciechanover A. The ubiquitin–proteasome proteolytic pathway: destruction for the sake of construction. Physiol Rev 2002;82:373–428.
[4] Powell SR. The ubiquitin–proteasome system in cardiac physiology and pathology. Am J Physiol Heart Circ Physiol 2006;291:H1–H19.
[5] Voges D, Zwickl P, Baumeister W. The 26S proteasome: a molecular machine designed for controlled proteolysis. Annu Rev Biochem 1999;68:1015–68.
[6] DeMartino GN, Slaughter CA. The proteasome, a novel protease regulated by multiple mechanisms. J Biol Chem 1999;274:22123–6.
[7] Tsukamoto O, Minamino T, Okada K, Shintani Y, Takashima S, Kato H, et al. Depression of proteasome activities during the progression of cardiac dysfunction in pressure-overloaded heart of mice. Biochem Biophys Res Commun 2006;340: 1125–33.
[8] Bulteau AL, Lundberg KC, Humphries KM, Sadek HA, Szweda PA, Friguet B, et al. Oxidative modification and inactivation of the proteasome during coronary occlusion/reperfusion. J Biol Chem 2001;276:30057–63.
[9] Zolk O, Schenke C, Sarikas A. The ubiquitin–proteasome system: focus on the heart. Cardiovasc Res 2006;70:410–21.
[10] Wang X, Robbins J. Heart failure and protein quality control. Circ Res 2006;99: 1315–28.
[11] Zong C, Gomes AV, Drews O, Li X, Young GW, Berhane B, et al. Regulation of murine cardiac 20S proteasomes: role of associating partners. Circ Res 2006;99:372–80.
[12] Zhang F, Hu Y, Huang P, Toleman CA, Paterson AJ, Kudlow JE. Proteasome function is regulated by cyclic AMP-dependent protein kinase through phosphorylation of Rpt6. J Biol Chem 2007;282:22460–71.
[13] Wang Z, Aris VM, Ogburn KD, Soteropoulos P, Figueiredo-Pereira ME. Prostaglandin J2 alters pro-survival and pro-death gene expression patterns and 26 S proteasome assembly in human neuroblastoma cells. J Biol Chem 2006;281: 21377–86.
[14] Fujita M, Asanuma H, Hirata A, Wakeno M, Takahama H, Sasaki H, et al. Prolonged transient acidosis during early reperfusion contributes to the cardioprotective effects of postconditioning. Am J Physiol Heart Circ Physiol 2007;292:H2004–8.
[15] Sanada S, Asanuma H, Tsukamoto O, Minamino T, Node K, Takashima S, et al. Protein kinase A as another mediator of ischemic preconditioning independent of protein kinase C. Circulation 2004;110:51–7.
[16] Sanada S, Kitakaze M, Papst PJ, Asanuma H, Node K, Takashima S, et al. Cardioprotective effect afforded by transient exposure to phosphodiesterase III inhibitors: the role of protein kinase A and p38 mitogen-activated protein kinase. Circulation 2001;104:705–10.
[17] Minamino T, Kitakaze M, Asanuma H, Tomiyama Y, Shiraga M, Sato H, et al. Endogenous adenosine inhibits P-selectin-dependent formation of coronary thromboemboli during hypoperfusion in dogs. J Clin Invest 1998;101: 1643–1653.
[18] Kitakaze M, Hori M, Sato H, Takashima S, Inoue M, Kitabatake A, et al. Endogenous adenosine inhibits platelet aggregation during myocardial ischemia in dogs. Circ Res 1991;69:1402–8.
[19] Ogita H, Node K, Asanuma H, Sanada S, Liao Y, Takashima S, et al. Amelioration of ischemia- and reperfusion-induced myocardial injury by the selective estrogen receptor modulator, raloxifene, in the canine heart. J Am Coll Cardiol 2002;40: 998–1005.
[20] Gomes AV, Zong C, Edmondson RD, Li X, Stefani E, Zhang J, et al. Mapping the murine cardiac 26S proteasome complexes. Circ Res 2006;99:362–71.
[21] Minamino T, Gaussin V, DeMayo FJ, Schneider MD. Inducible gene targeting in postnatal myocardium by cardiac-specific expression of a hormone-activated Cre fusion protein. Circ Res 2001;88:587–92.
[22] Powell SR, Wang P, Katzeff H, Shringarpure R, Teoh C, Khaliulin I, et al. Oxidized and ubiquitinated proteins may predict recovery of postischemic cardiac function: essential role of the proteasome. Antioxid Redox Signal 2005;7: 538–546.
[23] Satoh K, Sasajima H, Nyoumura KI, Yokosawa H, Sawada H. Assembly of the 26S proteasome is regulated by phosphorylation of the p45/Rpt6 ATPase subunit. Biochemistry 2001;40:314–9.
[24] Bose S, Stratford FL, Broadfoot KI, Mason GG, Rivett AJ. Phosphorylation of 20S proteasome alpha subunit C8 (alpha7) stabilizes the 26S proteasome and plays a role in the regulation of proteasome complexes by gamma-interferon. Biochem J 2004;378:177–84.
[25] Mutafova-Yambolieva VN, Smyth L, Bobalova J. Involvement of cyclic AMP-mediated pathway in neural release of noradrenaline in canine isolated mesenteric artery and vein. Cardiovasc Res 2003;57:217–24.
[26] Powell SR, Gurzenda EM, Teichberg S, Mantell LL, Maulik D. Association of increased ubiquitinated proteins with cardiac apoptosis. Antioxid Redox Signal 2000;2:103–12.
[27] Pye J, Ardeshirpour F, McCain A, Bellinger DA, Merricks E, Adams J, et al. Proteasome inhibition ablates activation of NF-kappa B in myocardial reperfusion and reduces reperfusion injury. Am J Physiol Heart Circ Physiol 2003;284: H919–26.
[28] Campbell B, Adams J, Shin YK, Lefer AM. Cardioprotective effects of a novel proteasome inhibitor following ischemia and reperfusion in the isolated perfused rat heart. J Mol Cell Cardiol 1999;31:467–76.

Journal of the American College of Cardiology
© 2009 by the American College of Cardiology Foundation
Published by Elsevier Inc.

Vol. 53, No. 8, 2009
ISSN 0735-1097/09/$36.00
doi:10.1016/j.jacc.2008.11.014

PRE-CLINICAL RESEARCH

Prolonged Targeting of Ischemic/Reperfused Myocardium by Liposomal Adenosine Augments Cardioprotection in Rats

Hiroyuki Takahama, MD,*†‡ Tetsuo Minamino, MD, PHD,§ Hiroshi Asanuma, MD, PHD,† Masashi Fujita, MD, PHD,§ Tomohiro Asai, PHD,¶ Masakatsu Wakeno, MD, PHD,*†‡ Hideyuki Sasaki, MD,*†‡ Hiroshi Kikuchi, PHD,# Kouichi Hashimoto,** Naoto Oku, PHD,¶ Masanori Asakura, MD, PHD,† Jiyoong Kim, MD,† Seiji Takashima, MD, PHD,§ Kazuo Komamura, MD, PHD,‖ Masaru Sugimachi, MD, PHD,‖ Naoki Mochizuki, MD, PHD,*‡ Masafumi Kitakaze, MD, PHD, FACC†

Osaka, Shizuoka, and Tokyo, Japan

Objectives The purpose of this study was to investigate whether liposomal adenosine has stronger cardioprotective effects and fewer side effects than free adenosine.

Background Liposomes are nanoparticles that can deliver various agents to target tissues and delay degradation of these agents. Liposomes coated with polyethylene glycol (PEG) prolong the residence time of drugs in the blood. Although adenosine reduces the myocardial infarct (MI) size in clinical trials, it also causes hypotension and bradycardia.

Methods We prepared PEGylated liposomal adenosine (mean diameter 134 ± 21 nm) by the hydration method. In rats, we evaluated the myocardial accumulation of liposomes and MI size at 3 h after 30 min of ischemia followed by reperfusion.

Results The electron microscopy and ex vivo bioluminescence imaging showed the specific accumulation of liposomes in ischemic/reperfused myocardium. Investigation of radioisotope-labeled adenosine encapsulated in PEGylated liposomes revealed a prolonged blood residence time. An intravenous infusion of PEGylated liposomal adenosine (450 μg/kg/min) had a weaker effect on blood pressure and heart rate than the corresponding dose of free adenosine. An intravenous infusion of PEGylated liposomal adenosine (450 μg/kg/min) for 10 min from 5 min before the onset of reperfusion significantly reduced MI size (29.5 ± 6.5%) compared with an infusion of saline (53.2 ± 3.5%, $p < 0.05$). The antagonist of adenosine A_1, A_{2a}, A_{2b}, or A_3 subtype receptor blocked cardioprotection observed in the PEGylated liposomal adenosine-treated group.

Conclusions An infusion as PEGylated liposomes augmented the cardioprotective effects of adenosine against ischemia/reperfusion injury and reduced its unfavorable hemodynamic effects. Liposomes are promising for developing new treatments for acute MI. (J Am Coll Cardiol 2009;53:709–17) © 2009 by the American College of Cardiology Foundation

Liposomes are now widely used for drug delivery in cancer treatment to target specific organs actively or passively and to prevent the degradation of chemotherapy agents (1). However, the application of liposomes for cardiovascular diseases is still limited. In ischemic/reperfused myocardium,

See page 718

cellular permeability is enhanced and vascular endothelial integrity is disrupted (2,3), suggesting that nanoparticles

*From the Department of Molecular Imaging in Cardiovascular Medicine, Osaka University Graduate School of Medicine, Osaka, Japan; †Department of Cardiovascular Medicine, National Cardiovascular Center, Osaka, Japan; ‡Department of Structural Analysis, Research Institute, National Cardiovascular Center, Osaka, Japan; §Department of Cardiovascular Medicine, Osaka University Graduate School of Medicine, Osaka, Japan; ‖Department of Cardiovascular Dynamics, Research Institute, National Cardiovascular Center, Osaka, Japan; ¶Department of Medical Biochemistry, School of Pharmaceutical Sciences, University of Shizuoka, Shizuoka, Japan; #Daiichi Pharmaceutical Co., Tokyo, Japan; and the **Daiichi-Sankyo Pharmaceutical Co., Tokyo, Japan. Supported by a grant for Scientific Research and a grant for the Advancement of Medical Equipment from the Japanese Ministry of Health, Labor, and Welfare, as well as a grant from the Japan Cardiovascular Research Foundation.

Manuscript received September 4, 2008; revised manuscript received October 21, 2008, accepted November 3, 2008.

Abbreviations and Acronyms

8-SPT = 8-(p-sulfophenyl) theophylline
EM = electron microscopy
MI = myocardial infarction
PEG = polyethylene glycol
RI = radioisotope
TTC = triphenyltetrazolium chloride

such as liposomes may be a promising drug delivery system for targeting damaged myocardium with cardioprotective agents. Additionally, coating liposomes with polyethylene glycol (PEG) prolongs their residence time in the circulation (1). Because enhanced microvascular permeability persists for at least 48 h after the occurrence of myocardial infarction (MI) (2), drugs delivered in PEGylated liposomes should be able to display their maximum beneficial effects on myocardial damage after MI.

Adenosine has multiple physiological functions that are mediated via the adenosine A_1, A_{2a}, A_{2b}, and A_3 receptors (4,5). Although large-scale clinical trials suggested the potential value of adenosine therapy for patients with acute MI (6,7), this agent has an extremely short half-life (1 to 2 s) and causes hypotension and bradycardia because of vasodilatory and negative chronotropic effects (4). Because a high dose of adenosine is required to exert cardioprotective effects, it is difficult to use clinically because of the associated hemodynamic consequences. Therefore, we hypothesized that adenosine encapsulated in PEGylated liposomes would cause less hemodynamic disturbance and might also specifically accumulate in ischemic/reperfused myocardium, leading to augmented cardioprotective effects. To test this hypothesis, we created PEGylated liposomal adenosine by the hydration method and investigated: 1) whether liposomal adenosine accumulated in ischemic/reperfused myocardium and prolonged blood residence time; 2) whether liposomal adenosine caused less severe hypotension and bradycardia than free adenosine; and 3) which adenosine receptor subtype was involved in mediating the cardioprotective effects of liposomal adenosine against ischemia/reperfusion injury.

Methods

Materials. The materials for preparing PEGylated liposomes, including hydrogenated soy phosphatidyl choline (HSPC), 1,2-distearoyl-sn-glycero-3-phosphoethanolamine-n-[methoxy (polyethylene glycol)-2000] (DSPE-PEG2000), and cholesterol were obtained from Nissei Oil Co., Ltd. (Tokyo, Japan) and Wako Pure Chemical Co., Ltd. (Osaka, Japan). [^{3}H]-adenosine was purchased from Daiichi Pure Chemicals Co., Ltd. (Tokyo, Japan). Other materials were obtained from Sigma (St. Louis, Missouri), including 8-(*p*-sulfophenyl)theophylline (8-SPT; a nonselective adenosine receptor antagonist), 1,3-diethyl-8-phenylxanthine (DPCPX; a selective adenosine A_1 receptor antagonist), 5-amino-7-(phenylethyl)-2-(2-furyl)-pyrazolo[4,3-e]-1,2,4-triazolo[1,5-c] pyrimidine (SCH58261; a selective adenosine A_{2a} receptor antagonist), 8-[4-[((4-cyanophenyl)carbamoylmethyl) oxy]phenyl]-1, 3-di(n-propyl)xanthine (MRS1754; a selective adenosine A_{2b} receptor antagonist), and 5-propyl-2-ethyl-4-propyl-3-(ethylsulfanylcarbonyl)-6-phenylpyridine-5-carboxylate (MRS1523, a selective adenosine A_3 receptor antagonist).

Animals. Male Wistar rats (9 weeks old and weighing 250 to 310 g, Japan Animals, Osaka, Japan) were used. The animal experiments were approved by the National Cardiovascular Center Research Committee and were performed according to institutional guidelines.

Preparation of PEGylated liposomes. The PEGylated liposomes were prepared by the hydration method. Briefly, adenosine was added to the lipid solution. After mixture of lipid and adenosine, DSPE-PEG2000 was added and incubated. The final composition of PEGylated liposomes was HSPC:cholesterol:DSPE-PEG2000 = 6.0:4.0:0.3 (molar ratio). After ultracentrifugation several times, the pellet of liposomal adenosine was resuspended in sodium lactate at each required concentration for use in the experimental protocols. Some samples of final liposomal adenosine were disrupted by dilution with 50% methanol (1.5 ml per 30-μl of liposomes). After 10 min of ultracentrifugation, the concentration of adenosine in the supernatant was measured by high-performance liquid chromatography.

To prepare fluorescent-labeled liposomes, 0.5 mol% tetramethylrhodamine isothiocyanate (rhodamine) was added to the lipid mixture. To prepare radioisotope (RI)-labeled adenosine encapsulated in liposomes, [^{3}H]-radiolabeled adenosine (Daiichi Pure Chemicals, Tokyo, Japan) was diluted with free adenosine and was encapsulated in liposomes as described above.

Characterization of PEGylated liposomal adenosine. The characterization of the liposomes was performed by the dynamic scatter analysis (Zetasizer Nano ZS, Malvern, Worcestershire, United Kingdom). The analyses were performed 10 times per sample, and results represented analyses of 4 independent experiments.

Experimental protocols. PROTOCOL 1: EFFECTS OF PEGYLATED LIPOSOMAL ADENOSINE ON HEMODYNAMICS IN RATS. Rats were anesthetized with intraperitoneal sodium pentobarbital (50 mg/kg). Catheters were advanced into a femoral artery and vein for the measurement of systemic blood pressure and infusion of drugs, respectively. Both blood pressure and heart rate were monitored continuously during the study using a Power Lab (AD Instruments, Castle Hill, Australia). After hemodynamics became stable, we intravenously administered empty PEGylated liposomes (n = 8), free adenosine (n = 8), or PEGylated liposomal adenosine (n = 8) for 10 min. Either PEGylated liposomal or free adenosine was infused at an initial dose of 225 μg/kg/min (0.1 ml/min) for 10 min. After a 5-min interval, either PEGylated liposomal adenosine or free adenosine was infused at 450 μg/kg/min (0.1 ml/min) for 10 min. In the same manner, PEGylated liposomal adenosine or free adenosine was then infused at 900 μg/kg/min (0.1 ml/min).

PROTOCOL 2: EFFECTS OF PEGYLATED LIPOSOMAL ADENOSINE ON INFARCT SIZE IN RATS. The MI was induced by transient ligation of the left coronary artery as described previously (8). In the first series of experiments, to examine the dose-dependent effects of liposomal adenosine on MI size, PEGylated liposomal adenosine was infused intravenously at 50, 150, or 450 μg/kg/min for a 10-min period starting from 5 min before the onset of reperfusion. In the second series of experiments, to determine the adenosine receptor subtype involved in cardioprotective effects by the liposomal adenosine, the antagonist of adenosine subtype receptor was intravenously injected as a bolus followed by the infusion of liposomal adenosine for 10 min. The MI size was evaluated at 3 h after the start of reperfusion. The doses of adenosine receptor subtype antagonists were determined according to the previous reports (9–11).

Measurement of infarct size. At 3 h after the onset of reperfusion, the area at risk and the infarcted area were determined by Evans blue and triphenyltetrazolium chloride (TTC) staining, respectively, as previously described (8). Infarct size was calculated as [infarcted area/area at risk] × 100(%) in a blind manner. The area at risk was composed of border (TTC staining) and infarcted (TTC nonstaining) areas.

Electron microscopy (EM). Myocardial samples for EM were obtained from the central and peripheral areas in ischemic/reperfused myocardium, which roughly corresponded to the infarcted and border areas, respectively, after the left coronary artery was occluded for 30 min of ischemia followed by 3 h of reperfusion. Samples were prepared as previously reported (12). Liposomes, whose major membrane component is unsaturated phospholipids, were visualized as homogenous dark dots with a diameter of 100 to 150 nm (13).

Accumulation of fluorescent-labeled PEGylated liposomes in ischemic/reperfused myocardium. Unlabeled or fluorescent-labeled PEGylated liposomes were infused intravenously at a dose of 0.1 ml/min as liposomal adenosine was infused in protocol 2. At 3 h after reperfusion, hearts were quickly removed and cut into 4 sections parallel to the axis from base to apex. Then ex vivo bioluminescence imaging was performed with an Olympus OV 100 imaging system (Olympus, Tokyo, Japan) and signals were quantified using WASABI quantitative software (Hamamatsu Photonics K.K., Shizuoka, Japan). Fluorescent intensity in the region of interest was measured as previously reported (14). Control intensity indicated the fluorescent intensity in the nonischemic area of the individual rat.

Time-course changes of free and PEGylated liposomal RI-labeled adenosine in plasma and myocardium. Free or PEGylated liposomal [^{3}H]-adenosine (83 kBq per rat) was infused intravenously at a dose of 0.1 ml/min as liposomal adenosine was infused in protocol 2. At the time indicated, rat hearts were harvested for counting of radioactivity (LSC-3100, Aloka Co., Tokyo, Japan). Results are expressed as a percentage of the injected dose per 1 ml of blood or 1 g of wet tissue weight.

Statistical analysis. The parameters of the liposomes were expressed as the average ± SD, whereas other data were expressed as the average ± SEM. Comparison of time-course changes in hemodynamic parameters between groups was performed by 2-way repeated-measures analysis of variance (ANOVA) followed by a post-hoc Bonferroni test. For comparison of RI activity between groups, statistical analysis was done with the Mann-Whitney *U* test. To address the differences in infarct size among groups, we performed a nonparametric (Kruskal-Wallis) test followed by evaluation with the Mann-Whitney *U* test. Resulting p values were corrected according to the Bonferroni method. To compare parameters of liposomes, an unpaired *t* test was performed. In all analyses, $p < 0.05$ was considered to indicate statistical significance.

Results

Characterization of liposomes by dynamic light scatter analysis. The dynamic light scatter analysis showed no significant difference in mean diameter, polydispersity index, or zeta-potential distribution between empty and adenosine-loaded PEGylated liposomes (Table 1).

Liposomes in ischemic/reperfused myocardium. The EM revealed the intact vascular endothelial cells and cardiomyocytes in the nonischemic myocardium (Figs. 1A and 1B). There were no homogenous dark dots indicating liposomes in the nonischemic myocardium of rats that received either saline (Fig. 1A) or liposomes (Fig. 1B). In the border area, many homogenous dark dots indicating liposomes were accumulated in rats that received liposomes, but not saline (Figs. 1C and 1D). In this area, significant structural damage was not observed in endothelium, but slight swelling of mitochondria was often observed. In the infarcted area, numerous liposomes were detected in rats that received liposomes, but not saline (Figs. 1E and 1F). In this area, the disrupted endothelial integrity and marked swelling of mitochondria were often observed.

Table 1 Characterization of Liposomes by Dynamic Light Scatter Analysis

	Mean Diameter (nm)	Polydispersity Index	Zeta Potential (mV)
PEGylated liposomes (empty liposomes)	126 ± 12	0.035 ± 0.003	−1.7 ± 0.4
PEGylated liposomal adenosine	134 ± 21	0.094 ± 0.002	−2.3 ± 1.1

Results represented analysis of 4 independent experiments. Values are expressed as mean ± SD.
PEG = polyethylene glycol.

JACC Vol. 53, No. 8, 2009
February 24, 2009:709–17

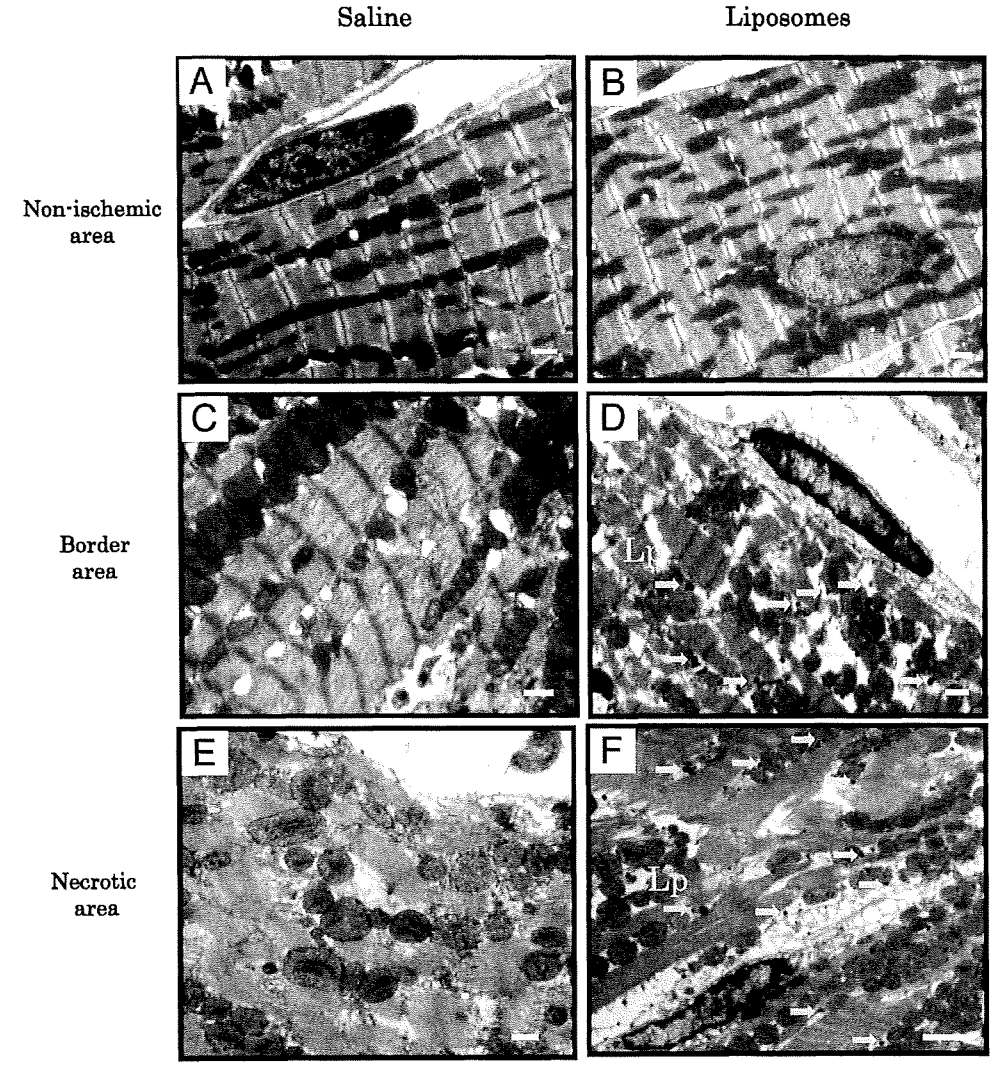

Figure 1 Liposomes in Ischemic/Reperfused Myocardium

(A, B) Representative electron micrographs of the nonischemic area in rats that received saline **(A)** or liposomes (Lp) **(B)**. **(C, D)** Representative electron micrographs of border area at 3 h after myocardial infarction (MI). Many **dark dots** accumulated in this area in the rat that received liposomes but not saline. **(E, F)** Representative electron micrographs of infarcted areas at 3 h after MI. Numerous **dark dots** accumulated in this area in the rat that received liposomes but not saline. Scale bars represent 1 μm.

Fluorescent-labeled PEGylated liposomes in ischemic/reperfused myocardium. Quantitative analysis by bioluminescence ex vivo bioluminescene imaging revealed that the target to control fluorescent intensity ratio was higher in the border (noninfarcted area at risk) as well as infarcted areas compared with a nonischemic one, suggesting that fluorescent-labeled liposomes were accumulated in the border as well as infarcted areas. Since there was no high-intensity area when unlabeled liposomes were infused, it was suggested that this was not a nonspecific phenomenon to MI by the ex vivo bioluminescence imaging system (Fig. 2). The Evans blue staining was unrelated to the fluorescence intensity (data not shown).

Plasma radioactivity of RI-labeled adenosine was markedly higher in the PEGylated liposomal adenosine group at 10 min and 3 h after the intravenous infusion than in the free adenosine group (Fig. 3A). Encapsulation within PEGylated liposomes also augmented the accumulation of adenosine in ischemic/reperfused myocardium compared with that of free adenosine (Fig. 3B).

Hemodynamic effects of PEGylated liposomal adenosine. Baseline hemodynamic parameters did not differ among the groups. An intravenous infusion of free adenosine at doses of 225, 450, and 900 μg/kg/min decreased the mean blood pressure by 14.8%, 25.4%, and 33.7%, respectively, compared with the effect of empty PEGylated lipo-

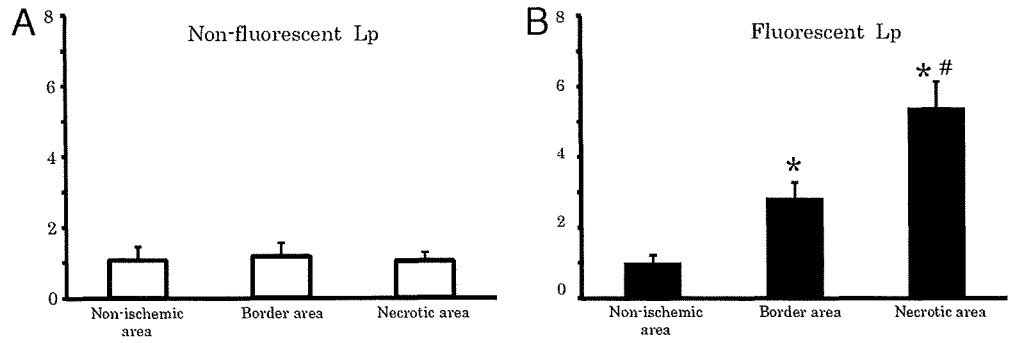

Figure 2 **Detection of Fluorescence-Labeled PEGylated Liposomes in Ischemic/Reperfused Myocardium**

Quantitative analysis of target-to-control fluorescent intensity ratio for each area in rats (n = 3 each group) that received nonfluorescent **(A)** or fluorescent **(B)** liposomes. The values of bioluminescence signals in the border and infarcted areas were expressed as the fold to that of the each nonischemic area. Values are expressed as the mean ± SEM (error bars). *p < 0.05 versus nonischemic areas. #p < 0.05 versus border areas.

somes. In contrast, the intravenous infusion of PEGylated liposomal adenosine at a dose of either 225 or 450 μg/kg/min did not significantly alter mean blood pressure (Fig. 4). Changes of the heart rate after infusion of PEGylated liposomal adenosine or free adenosine were similar to those observed for mean blood pressure (Fig. 4).

Effects of PEGylated liposomal adenosine on MI size. Baseline hemodynamic parameters were similar among all of the groups (Table 2). Intravenous infusion of free adenosine for 10 min reduced both the blood pressure and the heart rate, although these parameters returned to baseline within 5 min of ceasing infusion (Table 2). In contrast, hemodynamic parameters of the other groups were not altered (Table 2). The area at risk in the control group (61 ± 3%) did not differ compared with those of other groups that received liposomal adenosine. Intravenous infusion of PEGylated liposomal adenosine caused a dose-dependent decrease of MI size compared with that in the control group, whereas intravenous infusion of empty PEGylated liposomes or free adenosine did not (Fig. 5B).

The bolus injection of adenosine receptor antagonist did not alter the hemodynamic parameters (Table 3). The area at risk in the liposomal adenosine group (58 ± 3%) did not differ compared with those of other groups that received adenosine receptor antagonist. Infusion of 8-SPT, a nonspecific adenosine receptor antagonist, blunted the cardioprotective effect of liposomal adenosine (Fig. 6B). Furthermore, the infusion of the adenosine A_1, A_{2a}, A_{2b}, or A_3 receptor antagonist also blunted cardioprotective effects of liposomal adenosine (Fig. 6B). Infusion of 8-SPT alone did not significantly affect myocardial infarct size compared with the control (52 ± 5%, n = 4).

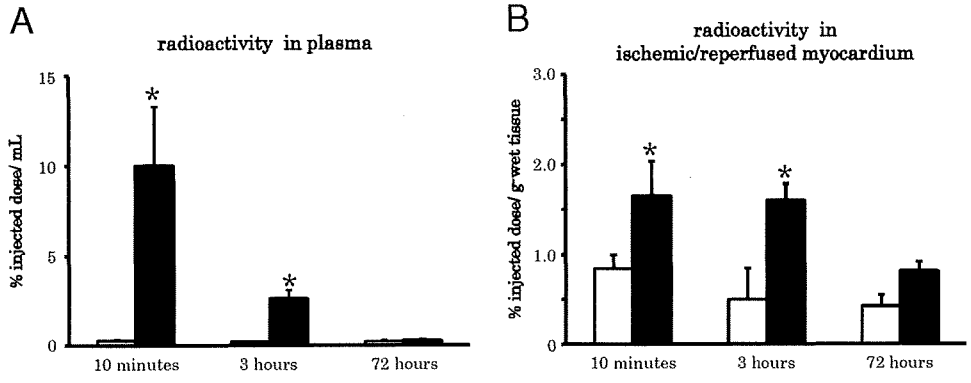

Figure 3 **Radioisotope-Labeled Adenosine in Plasma and Ischemic/Reperfused Myocardium**

(A) Changes in plasma radioactivity after infusion of radioisotope-labeled adenosine. **Solid and open bars** indicate the PEGylated liposomal adenosine and free adenosine groups, respectively (n = 4 each). In the PEGylated liposomal adenosine group, plasma radioactivity was markedly higher than in the free adenosine group. **(B)** Changes in radioactivity in ischemic/reperfused myocardium. **Solid and open bars** indicate the PEGylated liposomal adenosine and free adenosine groups, respectively (n = 4 each). In the PEGylated liposomal adenosine group, myocardial radioactivity was markedly higher than in the free adenosine group. Values are expressed as the mean ± SEM (error bars). *p < 0.05 versus the free adenosine group at the corresponding time.

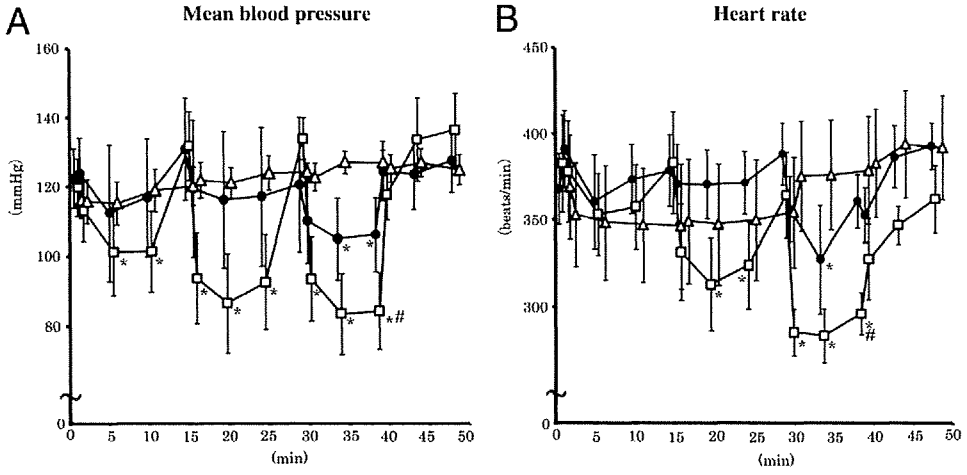

Figure 4 Hemodynamic Effects of PEGylated Liposomal Adenosine

Changes in the mean blood pressure **(A)** and heart rate **(B)** after intravenous infusion of various doses of empty PEGylated liposomes **(triangles)**, PEGylated liposomal adenosine **(circles)**, or free adenosine **(squares)** (n = 8 each). Values are expressed as the mean ± SEM. *p < 0.05 versus baseline at the corresponding group. #p < 0.05 versus PEGylated liposomes.

Discussion

In the present study, EM, bioluminescence ex vivo imaging, and fluorescent analysis revealed the accumulation of liposomes in the border (noninfarcted areas at risk) as well as infarcted ones, but not nonischemic myocardium, at 3 h after MI. These findings suggested that liposomes could specifically accumulate in ischemic/reperfused myocardium. Interestingly, EM revealed the existence of liposomes at sites where endothelial integrity was still morphologically maintained. Endothelial dysfunction such as enhanced permeability is induced by ischemic insult without morphological endothelial disruption (3,15). Enhanced permeability might lead to the accumulation of liposomes in the border as well as infarcted area, which will contribute to salvage the ischemic/reperfused myocardium. However, further investigation will be needed to determine the precise mechanism by which liposomes accumulate in ischemic/reperfused myocardium.

Analysis using RI-labeled adenosine encapsulated in liposomes revealed that plasma radioactivity was markedly higher in the PEGylated liposomal adenosine group compared with the free adenosine group. This indicates that encapsulation of adenosine by PEGylated liposomes considerably prolonged its residence time in the circulation and delayed its degradation. Consistent with the histological data, RI-labeled adenosine also showed preferential accumulation in ischemic/reperfused myocardium.

Table 2 Effects of Liposomal Adenosine on Hemodynamic Parameters

		Ischemia				Reperfusion	
	Baseline	0 min	15 min	25 min	30 min	5 min	10 min
Mean blood pressure (mm Hg)							
Saline	122 ± 5	102 ± 10	108 ± 7	107 ± 9	108 ± 7	105 ± 9	104 ± 9
Vehicle	127 ± 4	109 ± 8	108 ± 7	111 ± 9	111 ± 5	105 ± 5	103 ± 5
Free-Ado	124 ± 8	115 ± 8	111 ± 5	109 ± 4	66 ± 4*	62 ± 4*	112 ± 6
Lp-Ado 50 μg/kg/min	121 ± 5	106 ± 6	105 ± 6	110 ± 10	102 ± 6	101 ± 6	104 ± 4
Lp-Ado 150 μg/kg/min	122 ± 3	107 ± 6	107 ± 6	109 ± 11	105 ± 6	100 ± 6	103 ± 4
Lp-Ado 450 μg/kg/min	124 ± 3	104 ± 6	105 ± 6	107 ± 5	102 ± 6	99 ± 6	104 ± 4
Heart rate (beats/min)							
Saline	363 ± 22	366 ± 19	369 ± 14	413 ± 22	372 ± 12	372 ± 16	371 ± 14
Vehicle	363 ± 32	363 ± 6	383 ± 6	396 ± 25	367 ± 6	374 ± 7	372 ± 7
Free-Ado	360 ± 18	361 ± 17	384 ± 13	379 ± 18	305 ± 11*	293 ± 13*	356 ± 14
Lp-Ado 50 μg/kg/min	378 ± 19	386 ± 21	366 ± 12	376 ± 12	367 ± 19	369 ± 9	377 ± 17
Lp-Ado 150 μg/kg/min	388 ± 27	376 ± 20	371 ± 14	377 ± 13	378 ± 16	373 ± 16	369 ± 17
Lp-Ado 450 μg/kg/min	368 ± 17	376 ± 21	361 ± 13	386 ± 15	368 ± 15	363 ± 6	367 ± 7

Values are expressed as mean ± SEM. *p < 0.05 versus baseline.
Free-Ado = free adenosine; Lp-Ado = PEGylated liposomal adenosine; PEG = polyethylene glycol; vehicle = PEGylated liposomes.

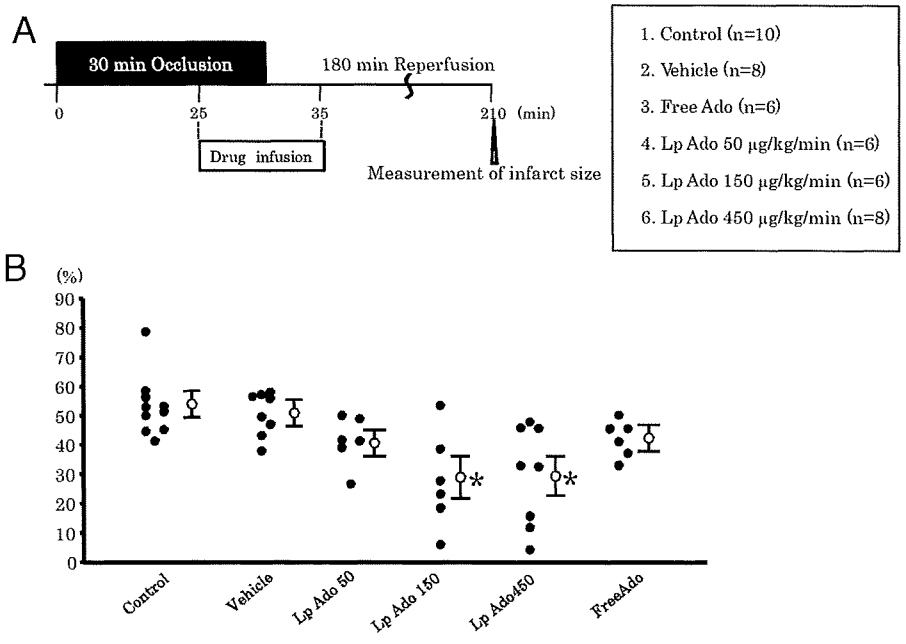

Figure 5 Dose-Dependent Effects of PEGylated Liposomal Adenosine on Myocardial Infarct Size

(A) Protocol showing the timing of infusion of PEGylated liposomal adenosine and of infarct size measurement. **(B)** Myocardial infarct size. Values are expressed as mean ± SEM (error bars). *$p < 0.05$ versus the control group. Free-Ado = free adenosine; Lp-Ado = PEGylated liposomal adenosine; Vehicle = PEGylated liposomes.

Furthermore, this study showed that PEGylated liposomal adenosine had a weaker effect on the blood pressure and heart rate than free adenosine. Thus, encapsulating adenosine in PEGylated liposomes attenuated its vasodilatory and negative chronotropic effects, presumably by reducing the amount of circulating free adenosine. However, the changes of hemodynamic parameters in this in vivo model suggested that significant release of adenosine from PEGylated liposomes would still occur if a large dose of liposomal adenosine (e.g., 900 μg/kg/min) were administered. Thus, further investigation of the in vivo pharmacodynamics of PEGylated liposomal adenosine is needed.

An intravenous infusion of PEGylated liposomal adenosine at the maximum dose that did not disturb hemodynamic parameters for 10 min before reperfusion reduced MI size in a dose-dependent manner, and this improvement was blocked by 8-SPT, a nonselective adenosine receptor antagonist. These findings suggest that adenosine released from liposomes acts via an adenosine receptor-dependent pathway. One possible mechanism by which PEGylated lipo-

Table 3 Effects of Adenosine Receptor Antagonist on Hemodynamic Parameters

		Ischemia				Reperfusion	
	Baseline	0 min	15 min	25 min	30 min	5 min	10 min
Mean blood pressure (mm Hg)							
Lp-Ado + 8SPT	120 ± 6	113 ± 4	112 ± 6	112 ± 5	107 ± 6	102 ± 8	109 ± 7
Lp-Ado + DPCPX	130 ± 6	105 ± 4	121 ± 4	100 ± 10	122 ± 6	120 ± 6	111 ± 4
Lp-Ado + SCH58261	132 ± 2	98 ± 12	99 ± 8	110 ± 8	118 ± 10	113 ± 10	109 ± 6
Lp-Ado + MRS1754	130 ± 3	95 ± 12	106 ± 8	105 ± 10	100 ± 10	96 ± 10	99 ± 7
Lp-Ado + MRS1523	130 ± 2	109 ± 8	104 ± 8	105 ± 9	100 ± 9	101 ± 10	104 ± 6
Heart rate (beats/min)							
Lp-Ado + 8SPT	404 ± 17	385 ± 10	374 ± 8	396 ± 8	389 ± 9	383 ± 8	385 ± 9
Lp-Ado + DPCPX	396 ± 24	380 ± 11	399 ± 9	398 ± 12	385 ± 9	382 ± 9	380 ± 7
Lp-Ado + SCH58261	393 ± 14	399 ± 15	381 ± 9	395 ± 15	376 ± 9	373 ± 9	385 ± 7
Lp-Ado + MRS1754	398 ± 14	392 ± 11	401 ± 9	379 ± 15	378 ± 9	374 ± 9	377 ± 7
Lp-Ado + MRS1523	396 ± 9	390 ± 11	390 ± 11	392 ± 10	373 ± 9	391 ± 7	388 ± 11

Values were expressed as mean ± SEM. *$p < 0.05$ versus baseline.
Lp-Ado = PEGylated liposomal adenosine; PEG = polyethylene glycol; Vehicle = PEGylated liposomes.

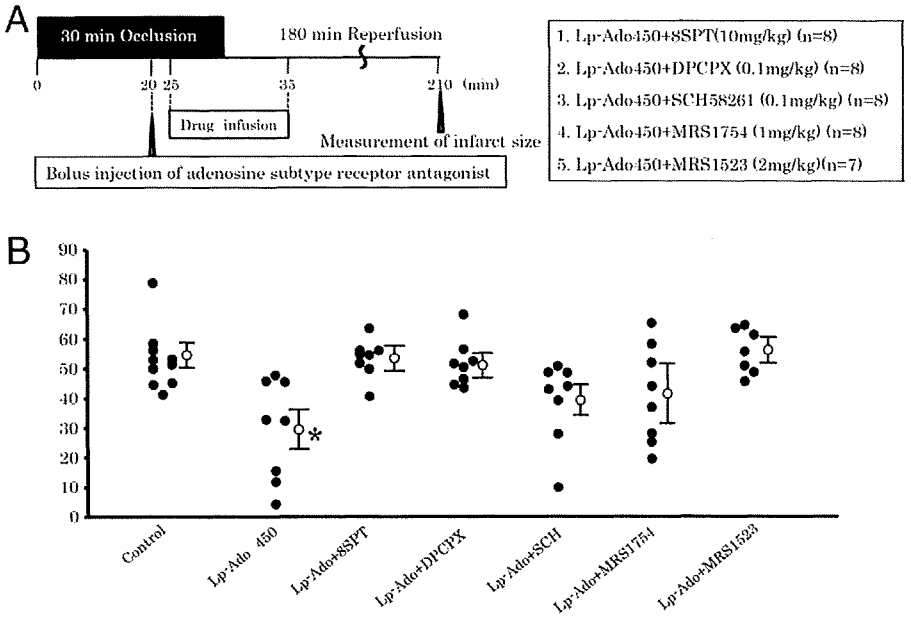

Figure 6 **Effects of Adenosine Receptor Antagonists on Myocardial Infarct Size**

(A) Protocol showing the timing of infusion of PEGylated liposomal adenosine and bolus injection adenosine receptor antagonists. **(B)** Myocardial infarct size. Values are expressed as the mean ± SEM (error bars). *$p < 0.05$ versus the control group. The abbreviations for adenosine antagonists were described in the text. Abbreviations as in Figure 5.

somes could augment cardioprotective effects of liposomal adenosine with minimum effects on hemodynamic parameters is the enhanced accumulation of PEGylated liposomal adenosine in ischemic/reperfused myocardium, which could augment various beneficial actions such as preventing calcium overload in the myocardium (5). The prolonged persistence of PEGylated liposomal adenosine would also increase its beneficial effect on ischemic/reperfused myocardium. Although continuous high-dose, long-term infusion of free adenosine was reported to reduce infarct size in rats (16), the present study did not confirm such a cardioprotective effect, probably because the total dose of free adenosine that we used was not high enough.

We found that myocardial infarct size in the group that received PEGylated liposomal adenosine with the antagonist of adenosine A_1, A_{2a}, A_{2b}, or A_3 subtype receptor was no different from the control group, indicating that every adenosine subtype receptor could possibly play a role in mediating cardioprotection by liposomal adenosine and that it was difficult to identify one particular subtype in the present study. Numerous studies reported that A_1, A_{2a}, A_{2b}, and A_3 receptors have been involved in cardioprotection against ischemia/reperfusion injury, and it remains controversial which adenosine subtype receptor is most responsible for cardioprotection (17–20). Furthermore, because the adenosine receptor antagonists used in the present study had some nonspecific effects, future investigation will be needed to examine the precise role of each adenosine receptor subtype using genetically engineered mice.

Because liposomal adenosine infused during reperfusion could reduce MI size, this agent could be a candidate for the adjunctive therapy of patients with acute MI. Importantly, adenosine is currently used for the diagnosis of ischemic heart disease and PEGylated liposomes are used to deliver anticancer agents (21). Thus, it should not be difficult to introduce PEGylated liposomal adenosine into clinical practice. Finally, PEGylated liposomes may provide a useful drug delivery system for targeting ischemic/reperfused myocardium with other agents.

Acknowledgments

The authors thank Akiko Ogai and Yoko Nakano for their excellent technical assistance; Motohide Takahama, Hiroyuki Hao, and Hatsue Ishibashi-Ueda for advice about the electron microscopy figure; and Syunichi Kuroda and Takashi Matsuzaki for assistance with bioluminescence imaging.

Reprint requests and correspondence: Dr. Tetsuo Minamino, Department of Cardiovascular Medicine, Osaka University Graduate School of Medicine, 2-2 Yamadaoka, Suita, Osaka 565-0871, Japan. E-mail: minamino@medone.med.osaka-u.ac.jp.

REFERENCES

1. Papahadjopoulos D, Allen TM, Gabizon A, et al. Sterically stabilized liposomes: improvements in pharmacokinetics and antitumor therapeutic efficacy. Proc Natl Acad Sci U S A 1991;24:11460–4.

2. Horwitz LD, Kaufman D, Keller MW, Kong Y. Time course of coronary endothelial healing after injury due to ischemia and reperfusion. Circulation 1994;90:2439–47.
3. Dauber IM, Van Benthuysen KM, McMurtry IF, et al. Functional coronary microvascular injury evident as increased permeability due to brief ischemia and reperfusion. Circ Res 1990;66:986–98.
4. Forman MB, Stone GW, Jackson EK. Role of adenosine as adjunctive therapy in acute myocardial infarction. Cardiovasc Drug Rev 2006;24:116–47.
5. Mubagwa K, Flameng W. Adenosine, adenosine receptors and myocardial protection: an updated overview. Cardiovasc Res 2001;52:25–39.
6. Mahaffey KW, Pume JA, Barbagelata NA, et al. Adenosine as an adjunct to thrombolytic therapy for acute myocardial infarction: results of a multicenter, randomized, placebo-controlled trial: the Acute Myocardial Infarction STudy of ADenosine (AMISTAD) trial. J Am Coll Cardiol 1999;34:1711–20.
7. Ross AM, Gibbons RJ, Stone GW, Kloner RA, Alexander RW, for the AMISTAD-II ÂInvestigators. A randomized, double-blinded, placebo-controlled multicenter trial of adenosine as an adjunct to reperfusion in the treatment of acute myocardial infarction (AMISTAD-II). J Am Coll Cardiol 2005;45:1775–80.
8. Bullard AJ, Govewalla P, Yellon DM. Erythropoietin protects the myocardium against reperfusion injury in vitro and in vivo. Basic Res Cardiol 2005;100:397–403.
9. Hannon JP, Tigani B, Wolber C, et al. Evidence for an atypical receptor mediating the augmented bronchoconstrictor response to adenosine induced by allergen challenge in activity sensitized Brown Norway rats. Br J Pharmacol 2002;135:685–96.
10. Kin H, Zatta AJ, Lofye MT, et al. Postconditioning reduces infarct size via adenosine receptor activation by endogenous adenosine. Cardiovasc Res 2005;67:124–33.
11. Hinschen AK, RoseMeyer RB, Headrick JP. Adenosine receptor subtypes mediating coronary vasodilation in rat hearts. J Cardiovasc Pharmacol 2003;41:73–80.
12. Kaeffeer N, Richard V, Francois A, Lallemand F, Henry JP, Thuillez C. Preconditioning prevents chronic reperfusion-induced coronary endothelial dysfunction in rats. Am J Physiol 1996;271:H842–9.
13. M Shimizu, Miwa K, Hashimoto Y, Goto A. Encapsulating of chicken egg yolk immunoglobulin G (IgY) by liposomes. Biosci Biotechnol Biochem 1993;57:1445–9.
14. Kasuya T, Jung J, Kadoya H, et al. In vivo delivery of bionanocapsules displaying phaseolus vulgaris agglutinin-L(4) isolectin to malignant tumors overexpressing N-acetylglucosaminlyltransferase V. Hum Gene Ther 2008;19:887–95.
15. Kim YD, Fomsgaard JS, Heim KF, et al. Brief ischemia-reperfusion induces stunning of endothelium in canine coronary artery. Circulation 1992;85:1473–82.
16. Canyon SJ, Dobson GP. Protection against ventricular arrhythmias and cardiac death using adenosine and lidocaine during regional ischemia in the in vivo rat. Am J Physiol Heart Circ Physiol 2004;287:H1286–95.
17. Yaar R, Jones MR, Chen JF, Ravid K. Animal models for the study of adenosineÂreceptor function. J Cell Physiol 2005;202:9–20.
18. Norton ED, Jackson EK, Turner MB, Virmani R, Forman MB. The effects of intravenous infusions of selective adenosine A_1-receptor and A_2-receptor agonists on myocardial reperfusion injury. Am Heart J 1992;123:332–8.
19. Xu Z, Mueller RA, Park SS, Boysen PG, Cohen MV, Downey JM. Cardioprotection with adenosine A_2 receptor activation at reperfusion. J Cardiovasc Pharmacol 2005;46:794–802.
20. Vinten-Johansen J. Postconditioning: a mechanical maneuver that triggers biological and molecular cardioprotective responses to reperfusion. Heart Fail Rev 2007;12:235–344.
21. Lasic DD. Doxorubicin in sterically stabilized liposomes. Nature 1996;380:561–2.

Key Words: myocardial infarction ■ liposome ■ drug delivery system ■ adenosine.

Available online at www.sciencedirect.com
ScienceDirect
Nuclear Medicine and Biology 36 (2009) 295–303
NUCLEAR MEDICINE — AND — BIOLOGY
www.elsevier.com/locate/nucmedbio

Evaluation of *O*-[^{18}F]fluoromethyl-D-tyrosine as a radiotracer for tumor imaging with positron emission tomography☆

Takeo Urakami[a], Koichi Sakai[b], Tomohiro Asai[a], Dai Fukumoto[b], Hideo Tsukada[b], Naoto Oku[a,*]

[a]*Department of Medical Biochemistry and Global COE, University of Shizuoka Graduate School of Pharmaceutical Sciences, Yada, Suruga-ku, Shizuoka 422-8526, Japan*

[b]*PET Center, Central Research Laboratory, Hamamatsu Photonics K.K., Hamamatsu, Shizuoka 434-8601, Japan*

Received 14 April 2008; received in revised form 3 December 2008; accepted 24 December 2008

Abstract

O-[^{18}F]Fluoromethyl-D-tyrosine (D-[^{18}F]FMT) has been reported as a potential tumor-detecting agent for positron emission tomography (PET). However, the reason why D-[^{18}F]FMT is better than L-[^{18}F]FMT is unclear. To clarify this point, we examined the mechanism of their transport and their suitability for tumor detection. The stereo-selective uptake and release of enantiomerically pure D- and L-[^{18}F]FMT by rat C6 glioma cells and human cervix adenocarcinoma HeLa cells were examined. The results of a competitive inhibition study using various amino acids and a selective inhibitor for transport system L suggested that D-[^{18}F]FMT, as well as L-[^{18}F]FMT, was transported via system L, the large neutral amino acid transporter, possibly via LAT1. The in vivo distribution of both [^{18}F]FMT and [^{18}F]FDG in tumor-bearing mice and rats was imaged with a high-resolution small-animal PET system. In vivo PET imaging of D-[^{18}F]FMT in mouse xenograft and rat allograft tumor models showed high contrast with a low background, especially in the abdominal and brain region. The results of our in vitro and in vivo studies indicate that L-[^{18}F]FMT and D-[^{18}F]FMT are specifically taken up by tumor cells via system L. D-[^{18}F]FMT, however, provides a better tumor-to-background contrast with a tumor/background (contralateral region) ratio of 2.741 vs. 1.878 with the L-isomer, whose difference appears to be caused by a difference in the influence of extracellular amino acids on the uptake and excretion of these two isomers in various organs. Therefore, D-[^{18}F]FMT would be a more powerful tool as a tumor-detecting agent for PET, especially for the imaging of a brain cancer and an abdominal cancer.

Keywords: *O*-[^{18}F]Fluoromethyl tyrosine; D-isomer; Positron emission tomography (PET); System L transporter; Tumor imaging

1. Introduction

[^{18}F]FDG is the most widely used tracer for tumor detection with PET imaging. However, several limitations with [^{18}F]FDG have been reported, such as a high uptake in normal brain and heart and in inflammatory tissues [1]. In contrast, the accumulation of positron emitter-labeled amino acids was assumed to reflect enhanced amino acid transport, metabolism and protein synthesis. Therefore, these amino acid tracers have been used for detecting tumors especially those in the brain.

Positron emitter-labeled amino acids and their derivatives, such as 1-[^{11}C]methionine [2], methyl-[^{11}C]methionine [2,3], 1-[^{11}C]tyrosine [4], 1-[^{11}C]leucine [5], 1-[^{11}C]phenylalanine [6], 4-[^{18}F]fluoro-phenylalanine [7] and 2-[^{18}F]fluoro-L-tyrosine [8], have been proposed as PET imaging agents. Among these positron emitter-labeled amino acids, [^{11}C]methionine is widely used for tumor imaging with PET. Recently, several amino acid analogs, namely, *O*-[^{11}C]methyl-L-tyrosine [9], *O*-[^{18}F]fluoromethyl-L-tyrosine (L-[^{18}F]FMT) [9], *O*-[^{18}F]fluoroethyl-L-tyrosine [10,11], *O*-[^{18}F]fluoropropyl-L-tyrosine [12,13], [^{11}C]ethyonine [14] and [^{11}C]propionine [14], were synthesized and evaluated as PET imaging agents. These amino acid

☆ This study was supported by a grant from the Central Shizuoka Cooperation of Innovative Technology and Advanced Research in Evolution Area (City Area) supported by the Ministry of Education, Culture, Sports, Science and Technology of Japan (MEXT); and also by the Research and Development of Technology for Measuring Vital Function Merged with Optical Technology, MEXT; and by the Research and Development Project Aimed at Economic Revitalization, MEXT.

* Corresponding author. Tel.: +81 54 264 5701; fax: +81 54 264 5705.
E-mail address: oku@u-shizuoka-ken.ac.jp (N. Oku).

0969-8051/$ – see front matter © 2009 Published by Elsevier Inc.
doi:10.1016/j.nucmedbio.2008.12.012

analogues showed relatively low accumulation in normal peripheral tissue (low tissue-to-blood ratio), rapid blood clearance and a rather high amount of label remaining in tumor tissues (high tumor-to-blood ratio).

In contrast to L-isomers of amino acids, D-isomers are considered to behave as unnatural amino acids, like the amino acid analogs mentioned above. In previous reports in the 1980s, in vivo and in vitro experiments using ^{14}C-labeled D-amino acids revealed that the accumulation of D-isomers was higher than that of L-isomers in tumor cells [15,16]. At that time, the potential of D-isomers of amino acids as nuclear imaging agents was mentioned [15–17]. However, the precise mechanism responsible for the higher accumulation of the D-isomers has remained unclear. Recently, the biological functions of D-isomers in the central nervous system [18], developmental biology [19] and some pathological conditions [20,21] were reported, although the precise behavior of D-isomers still remains to be clarified [22].

Amino acid transport across the plasma membrane is mediated via amino acid transporters located on the membrane. Among the amino acid transport systems, system L, a Na^+-independent neutral amino acid transporter system, is the major route for providing cells with large neutral amino acids including branched or aromatic amino acids [23]. Recently, system L amino acid transporters 1 and 2 (LAT1 and LAT2) were isolated, and their characteristics were evaluated [24–26]. LAT1 was shown to be strongly expressed in malignant tumors [27,28] and also expressed in some normal organs such as brain, spleen, placenta and testis [29]. In contrast, the distribution of LAT2 mRNA is ubiquitous [30,31]. We previously reported that the D-isomer of *O*-[^{18}F]fluoromethyl-L-tyrosine (D-[^{18}F]FMT) was highly accumulated in tumor tissue [32,33], although the accumulation of D-[^{18}F]FMT in normal tissues, e.g., brain, kidney and pancreas, was low as was the whole-body background. However, the molecular mechanism of D-[^{18}F]FMT uptake in tumor tissue was not addressed at that time. Since the presence of amino acids in plasma would affect the uptake of this tracer into tissues, the concentrations of amino acids in plasma, in normal and tumor tissues, and in the microenvironment of tumor cells must be considered [34].

In this study, the characteristics and utility of the D-isomer of an artificial amino acid labeled with ^{18}F positron emitter were evaluated; and the behavior of L-[^{18}F]FMT and D-[^{18}F]FMT both in vitro and in vivo was examined.

2. Materials and methods

2.1. Materials

L-Alanine, L-glycine, L-phenylalanine, L-serine, D-leucine and L-leucine were purchased from Wako Pure Chemical Co. Ltd. (Osaka, Japan). 2-Aminobicyclo-(2,2,1)-heptane-2-carboxylic acid (BCH) was obtained from Sigma-Aldrich Japan (Tokyo, Japan). All other reagents were of analytical grade.

2.2. Synthesis of labeled compound

Positron-emitting ^{18}F was produced by ^{18}O(p,n)^{18}F nuclear reaction using the cyclotron (HM-18; Sumitomo Heavy Industry, Japan) at Hamamatsu Photonics PET Center. L- and D-Isomers of [^{18}F]FMT were synthesized by reacting [^{18}F]fluoro-methyl bromide with the corresponding L- and D-tyrosine according to a previous report [32,33]. Enantiomeric purity was analyzed on a CHIOBIOTIC T column (4.6×250 mm; Tokyo Kasei Kogyo). The elution solution was ethanol/water (1:1), and the flow rate was 1 ml/min. The production of [^{18}F]FDG was performed according to the method reported previously [35]. Specific activities of D-[^{18}F]FMT, L-[^{18}F]FMT and [^{18}F]FDG were 115±10, 126±12 and 144±21 GBq/μmol, respectively; and radiochemical purities were 99.6±0.4%, 99.8±0.3% and 100.0±0.0%, respectively.

2.3. Cell culture

C6 glioma cells (ATCC, Rockville, MD, USA) and HeLa cells (RIKEN, Tsukuba, Japan) were grown in Dulbecco's Modified Eagle's Medium (DMEM, Wako) supplemented with 10% fetal bovine serum (Japan Bioserum, Hiroshima, Japan) and appropriate concentrations of antibiotics (100 U/ml penicillin and 100 μg/ml streptomycin). The cells were maintained in plastic culture flasks at 37°C in a humidified atmosphere containing 5% CO_2 and kept as monolayers.

2.4. Measurement of uptake by cells in culture

Rat C6 glioma cells and HeLa cells were plated in 24-well culture plates (Corning Japan, Tokyo, Japan) at a density of 2×10^5 cells per well and cultured for 24 h. After the growth medium had been removed, the cells were washed twice with Hank's balanced salt solution (HBSS; 136.6 mM NaCl, 5.4 mM KCl, 4.2 mM $NaHCO_3$, 1 mM $CaCl_2$, 0.5 mM $MgCl_2$, 0.44 mM KH_2PO_4 and 0.41 mM $MgSO_4$) and kept in HBSS for 30 min at 37°C to deplete any residual nutrients from the growth medium. Then the HBSS was discarded, and the uptake assay was started by adding a trace amount of D- or L-isomer of [^{18}F]FMT/HBSS (1–3 MBq/ml) to the cultures. After incubation for the selected time period (2, 5, 10, 30 and 60 min), the uptake of labeled compounds was terminated by removing the medium. After the cells had been washed twice with 1 ml of ice-chilled Dulbecco's phosphate-buffered saline (PBS), the cells were lysed in 400 μl of cell lysis solution (0.1 M NaOH, 2% Triton X-100). The radioactivity in the cell lysates was measured by a γ-counter (Aloka ARC-2000). More than three independent experiments, each done in triplicate, were performed.

2.5. Tracer release from cultured cells

Experiments were performed using 24-well culture plates. HeLa cells (2×10^5 cells/well) were incubated with D- or L-isomer of [^{18}F]FMT (1-3 MBq/ml) in HBSS for 30 min at 37°C. Then, the cells were washed three times with HBSS, and all supernatants were discarded. Release experiments were started by the addition of 1 ml HBSS. The supernatant

was collected at each time point from each well, and cells in the well were washed twice with ice-chilled PBS very quickly. Then the cells were lysed with 400 μl of cell lysis solution (0.1 M NaOH, 2% Triton X-100), and the radioactivity in the cell lysates was measured by a γ-counter. More than three independent experiments, each done in triplicate, were performed.

2.6. Reverse transcriptase–polymerase chain reaction

Total RNAs were isolated from C6 glioma and HeLa cells by using an RNA purification kit (QIAshredder and RNeasy kit, QIAGEN KK, Tokyo, JAPAN) in accordance with the manufacturer's instructions. Then, the first-strand cDNAs were prepared with a Superscript First-strand Synthesis system (Invitrogen Japan KK, Tokyo, Japan) and oligo(dT) primer, and used as a template for polymerase chain reaction (PCR) amplification. The PCR amplification was performed with Ex Taq (Takara Bio, Inc., Ohtu, Japan) according to the following protocol [27]: 94°C for 5 min, followed by 25 cycles of 94°C for 30 s, 60°C for 30 s and 72°C for 1 min and a final extension step of 72°C for 10 min. The following primer pairs were used for PCR amplification: 5′-CAATGGTGTGGCCATCATG-3′ and 5′-GATGCATCCCCTTGTCCTAT-3′ for rat LAT1, 5′-TCATTGGCTCCGGAATCTTC-3′ and 5′-ATGCA TTCTTTGGCTCCAGC-3′ for rat LAT2, 5′-TCACAGGCT-TATCCAAGGAG-3′ and 5′-TACAATGTCAGCCTGAG-GAG-3′ for rat 4F2hc, 5′-TTCATCGCA- GTACATCG-TGG-3′ and 5′-CCCAGGTGATAGTTCCCGAA-3′ for human LAT1, 5′-AGCCCTGAAGAAAGAGATCG-3′ and 5′-TGCATATCTGTACAATCCCC-3′ for human LAT2, 5′-TCGATTACCTGAGCTCTCTG-3′ and 5′-GGGATTTTG-TATGCTCCCCA-3′ for human 4F2hc and 5′-TGACGGGGTCACCCACACTGTGCCCATCTA-3′ and 5′-CTAGAAGCATTTGCGGTGGACGATGGAGGG-3′ for human and rat β-actin.

2.7. Animals

All animals were maintained and handled in accordance with the recommendations of the National Institutes of Health and the Animal Facility Guidelines of the University of Shizuoka.

The mice bearing tumors were prepared as reported previously [32]. Briefly, female BALB/cA Jcl-nu mice (7 weeks old) were inoculated subcutaneously with 5×10^6 HeLa cells, maintained for 2 weeks after the transplantation and used for experiments at 9 weeks of age.

Male Fischer rats (9 weeks old) were obtained from Japan SLC, Inc. The rat C6 brain tumor model was prepared as reported elsewhere with a minor modification [36]. Rats were anesthetized with chloral hydrate and individually placed in a stereotaxic apparatus. C6 glioma cells (2×10^5 cells/10 μl of DMEM containing 1% gelatin) were injected at a rate of 1.0 μl/min into the left hippocampus of the rat (−4.7 mm posterior to bregma, −3.9 mm lateral to the midline suture and −6.2 mm from the dura) via a 28-gauge stainless tube. Eleven days after tumor implantation, the rats were used for PET studies.

2.8. Whole-body imaging of tumor-bearing mice and rats

The distribution pattern of each radiolabeled compound in the rats was determined with a small-animal PET system (Clairvivo PET, Shimadzu, Kyoto, Japan). Animals were anesthetized by an intraperitoneal injection of chloral hydrate at 400 mg/kg, followed by continuous infusion of the anesthetic at 100 mg/kg per hour through a cannula placed into a tail vein. Anesthetized rats were fixed on an animal holder. Each ^{18}F-radiolabeled compound at a dose of 7 MBq was injected intravenously into each rat via a tail vein. The data were obtained with a list mode data acquisition every 1 s for 60 min. Reconstruction was made by 3D-DRAMA (two iterations, γ=0.1) with resolution modeling. After the PET analysis, the rat brains were excised and sliced into eight coronal slices of 2-mm thickness (four slices anterior to and four slices posterior to the optical chiasm) with a brain slicer (Muromachi Kikai, Co. Ltd, Tokyo, Japan). The distribution of [^{18}F]FMT or [^{18}F]FDG in each brain slice was determined by autoradiography after exposure to an imaging plate for approximately 1 h. The autoradiograms of the brain slices were obtained by using a Bio-imaging analyzer BAS1500 and analyzed by Image Gauge V3.45 (Fuji Photo Film, Co. Ltd, Tokyo, Japan).

3. Results

3.1. Uptake and release of [^{18}F]FMT in vitro

The enantiomeric purity of each isomer was determined by the enantiomeric analytic HPLC as reported previously [33]. The results showed the enantiomeric purity of each isomer to be more than 98%.

At first, we examined the transport of the D- and L-isomers of [^{18}F]FMT in rat C6 glioma cells and HeLa cells. The uptake of D- and L-isomers of [^{18}F]FMT into these cells was measured at selected time points up to 30 min. As a result, the uptake rate of the L-isomer was significantly higher than that of the D-isomer in both C6 glioma and HeLa cells (Fig. 1). The uptake was not saturated at least up to 60 min (data not shown).

Then, the release of the D- and L-isomers from HeLa cells in the presence or absence of 100 μM L-leucine was examined. As shown in Fig. 2A, the release of the D-isomer under the amino acid-free condition in HBSS was slower than that of L-isomer. On the other hand, the release rate of both L-[^{18}F]FMT and D-[^{18}F]FMT was accelerated in the presence of L-leucine (Fig. 2B). These uptake and release experimental results on [^{18}F]FMT indicate that the amino acid transport activity of the D-isomer was lower than that of the L-isomer in both C6 glioma and HeLa cells in vitro. Then, we further examined the selectivity of the transporter by performing inhibition experiments in C6 glioma cells. The uptake of D- and L-isomers of [^{18}F]FMT was strongly inhibited in the presence of 1 mM L-isomers of methionine, phenylalanine and tyrosine (Fig. 3A). The uptake was also

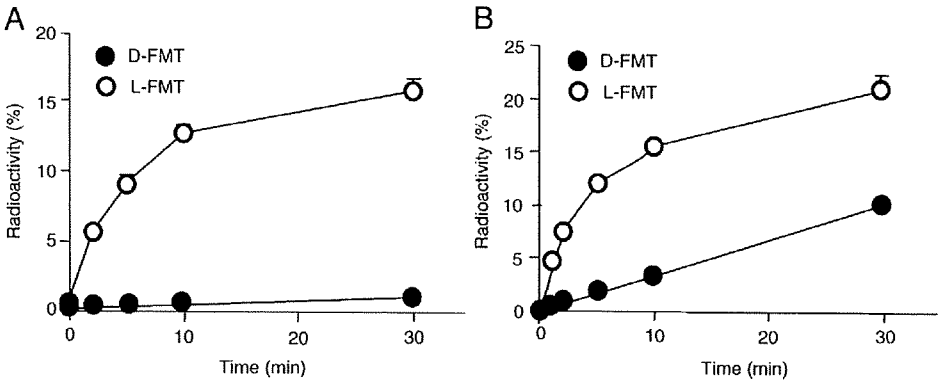

Fig. 1. Time-dependent uptake of D- and L-isomers of [^{18}F]FMT by C6 glioma and HeLa cells. The C6 glioma (A) and HeLa (B) cells were incubated for 1, 2, 5, 10 or 30 min in uptake solution containing 1–3 MBq of D- or L-isomers of [^{18}F]FMT. The relative radioactivity (as a percentage of the total dose) at each point is indicated as the mean±S.D. More than three independent experiments, each done in triplicate, were performed.

inhibited by BCH, a selective inhibitor of the system L amino acid transporter. However, the uptake was not inhibited by L-glycine. These inhibition patterns in the presence of amino acids for uptake of D- and L-isomers of [^{18}F]FMT were essentially the same, suggesting that both D- and L-isomers of [^{18}F]FMT were taken up by the same transporter, namely, the system L amino acid transporter.

Since the activity of the system L amino acid transporter is reported to be independent of extracellular sodium ions [24,25], we next examined the sodium ion dependency of the D- and L-[^{18}F]FMT transport. A sodium ion-free condition was obtained by substitution of sodium chloride with choline chloride, as reported previously [25]. Fig. 3B shows the sodium ion-independent uptake of both D- and L-isomers. These results support the idea that both D- and L- isomers of [^{18}F]FMT are transported by system L amino acid transporters.

Next, the effect of the competitive inhibition of the system L amino acid transporter on the uptake of D- or L-isomer of [^{18}F]FMT was examined. D-[^{18}F]FMT or L-[^{18}F]FMT was loaded into HeLa cells in the presence of the various concentrations of BCH, a selective inhibitor of system L (Fig. 4A). The uptake of both D- and L-isomers of [^{18}F]FMT was inhibited by BCH in a dose- dependent manner. Furthermore, the inhibitory effect of various concentrations of natural amino acids, i.e., D- and L-leucine, on isomer uptake was examined. Both D- and L-leucine inhibited the uptake of [^{18}F]FMT; however, L-[^{18}F]FMT uptake was decreased more at a low concentration of the extracellular amino acids (Fig. 4B and C) than the D-isomer. These results suggest that the transport of L-[^{18}F]FMT was more affected in the presence of either L-leucine or D-leucine than that of the D-isomer in vitro and that this might also be the case in vivo.

System L amino acid transporter proteins LAT1 and LAT2 were isolated previously. LAT1 and LAT2 require an additional single-membrane-spanning protein heavy chain of the 4F2 antigen (4F2hc) for their functional expression in the plasma membrane. LAT1 and 4F2hc or LAT2 and 4F2hc form a heterodimeric complex via a disulfide bond. So we examined the mRNA expression of the system L amino acid transporters in C6 glioma and HeLa cells. In the reverse

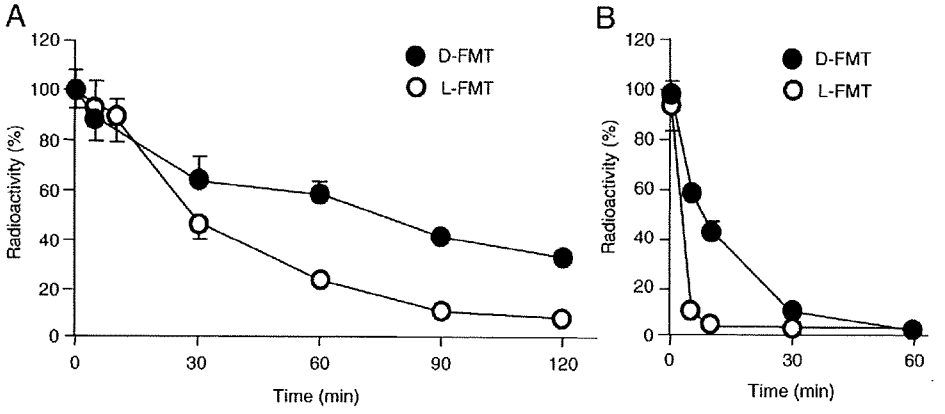

Fig. 2. Release of D- and L-isomers of [^{18}F]FMT preloaded in HeLa cells. The release of preloaded [^{18}F]FMT from HeLa cells was examined. The cells preloaded with D- or L-isomers of [^{18}F]FMT were incubated in the absence (A) or presence (B) of 100 μM L-leucine. The relative radioactivities that remained in the cells were determined to obtain the release rate of [^{18}F]FMT. Each point indicates the mean±S.D. More than three independent experiments, each carried out in triplicate, were performed.

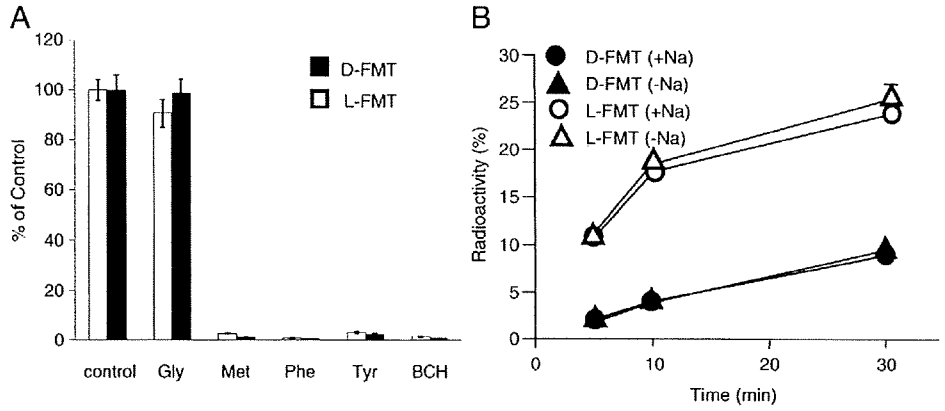

Fig. 3. Uptake of D- and L-isomers of [^{18}F]FMT by C6 glioma cells in the presence of amino acids, inhibitors and Na^+ ions. (A) C6 glioma cells were incubated with D- or L-isomer of [^{18}F]FMT in the uptake solution containing L-glycine, L-methionine, L-phenylalanine, L-tyrosine or BCH (100 μM for each). The relative radioactivity in the cells was determined. (B) C6 glioma cells were incubated with D- or L-isomer of [^{18}F]FMT in the uptake solution in the presence (circles) or absence (triangles) of Na^+ ions. The relative radioactivity of cells was determined. Data are presented as the relative mean±S.D.

transcriptase–PCR (RT-PCR) analysis, the PCR products for LAT1 and their associating protein 4F2hc, but not the LAT2 product, were detected when RNA from the rat C6 glioma and HeLa cell cultures was used (Fig. 5).

3.2. Tumor PET imaging with [^{18}F]FMT

Noninvasive real-time imaging with a small-animal PET provides distribution data consistent with those obtained from tissue dissection assays. Mice xenografted with HeLa cells were prepared and examined by PET. Data were acquired from mice administered D-[^{18}F]FMT, L-[^{18}F]FMT or [^{18}F]FDG (Fig. 6). The mouse injected with D-[^{18}F]FMT showed the clearest difference in tracer intensity between the tumor (right leg) and the normal tissue (left leg) compared with the mice given the other tracers. The accumulation of D-[^{18}F]FMT in the tumor tissue was not different from that of L-[^{18}F]FMT. The standard uptake value (SUV) of the former was 1.336; and that of the latter, 1.642. However,

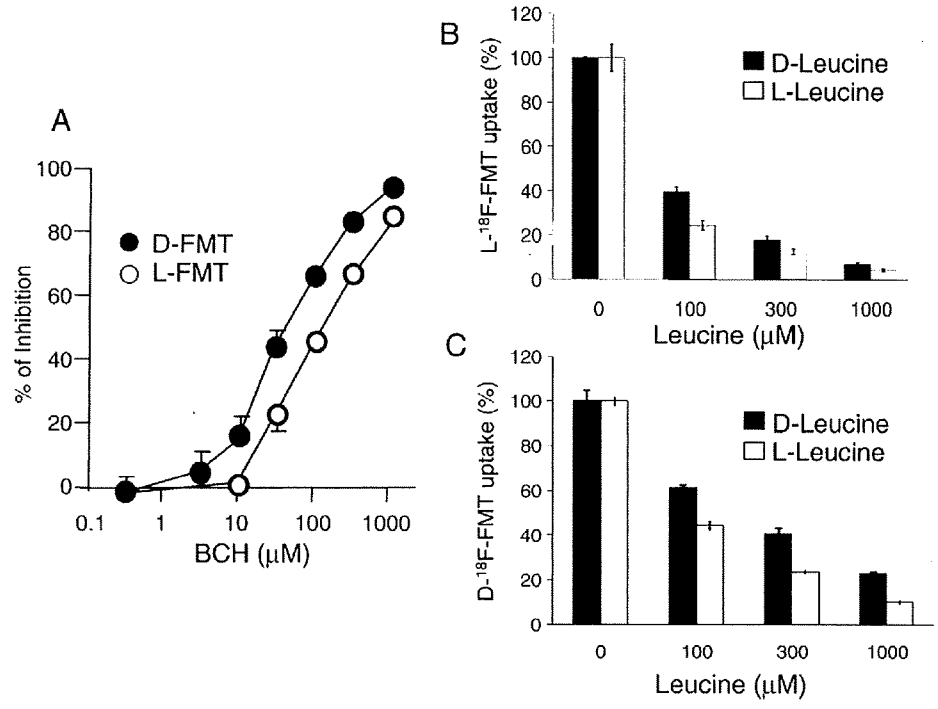

Fig. 4. BCH- and L- or D-leucine-mediated inhibition of D- or L-[^{18}F]FMT uptake by HeLa cells. The uptake of D- (open circle) or L-isomer (closed circle) of [^{18}F]FMT was measured for 5 min in the presence of various concentrations of BCH (A). The stereo-selective inhibitory effect of leucine on the uptake of L-[^{18}F]FMT (B) and D-[^{18}F]FMT (C) into HeLa cells was examined in the presence of 0, 100, 300 and 1000 μM L- or D-leucine. The graph shows the % radioactivity of the control (without leucine). Bars indicate the mean±S.D.